

1   **An antisense RNA capable of modulating the  
2   expression of the tumor suppressor microRNA-34a**

3  
4   **Jason T. Serviss<sup>1\*</sup>, Felix Clemens Richter<sup>1,2</sup>, Jimmy Van den Eynden<sup>3</sup>,**  
5   **Nathanael Johansson Andrews<sup>1</sup>, Miranda Houtman<sup>1,4</sup>, Mattias**  
6   **Vesterlund<sup>1</sup>, Laura Schwarzmüller<sup>1,5</sup>, Per Johnsson<sup>6,7</sup>, Erik Larsson<sup>3</sup>,**  
7   **Dan Grandér<sup>1</sup>, Katja Pokrovskaia Tamm<sup>1</sup>**

8  
9   <sup>1</sup> Department of Oncology and Pathology, Karolinska Institutet, Stockholm, Sweden, SE-  
10   17177

11   <sup>2</sup> Kennedy Institute of Rheumatology, University of Oxford, Roosevelt Drive, Oxford OX3 7FY,  
12   UK

13   <sup>3</sup> Department of Medical Biochemistry and Cell Biology, Institute of Biomedicine, The  
14   Sahlgrenska Academy, University of Gothenburg, SE-405 30 Gothenburg, Sweden

15   <sup>4</sup> Rheumatology Unit, Department of Medicine, Karolinska University Hospital Solna,  
16   Karolinska Institutet, Stockholm, Sweden

17   <sup>5</sup> Laboratory for Experimental Oncology and Radiobiology (LEXOR), Center for Experimental  
18   Molecular Medicine (CEMM), Academic Medical Center, Amsterdam, The Netherlands

19   <sup>6</sup> Ludwig Institute for Cancer Research, Stockholm, Sweden

20   <sup>7</sup> Department of Cell and Molecular Biology, Karolinska Institutet, Stockholm, Sweden

21  
22   **\* Correspondence:**

23   Jason T. Serviss [jason.serviss@ki.se](mailto:jason.serviss@ki.se)

24  
25   **Abstract**

26  
27   The microRNA-34a is a well-studied tumor suppressor microRNA (miRNA)  
28   and a direct downstream target of TP53 and has roles in several pathways  
29   associated with oncogenesis, such as proliferation, cellular growth, and  
30   differentiation. Due to its broad tumor suppressive activity, it is not surprising  
31   that *miR34a* expression is altered in a wide variety of solid tumors and  
32   hematological malignancies. However, the mechanisms by which *miR34a* is  
33   regulated in these cancers is largely unknown. In this study, we find that a  
34   long non-coding RNA transcribed antisense to the *miR34a* host gene, is  
35   critical for *miR34a* expression and mediation of its cellular functions in multiple  
36   types of human cancer. In addition, we characterize *miR34a* antisense RNA's  
37   ability to facilitate *miR34a* expression under different types of cellular stress in  
38   both *TP53* deficient and wildtype settings.

40

41 **Introduction**

42 In recent years advances in functional genomics has revolutionized our  
43 understanding of the human genome. Evidence now points to the fact that  
44 approximately 75% of the genome is transcribed but only ~1.2% of this is  
45 responsible for encoding proteins (International Human Genome Sequencing  
46 2004, Djebali et al. 2012). Of these recently identified elements, long non-  
47 coding (lnc) RNAs are defined as transcripts exceeding 200 base pairs (bp) in  
48 length with a lack of a functional open reading frame. Some lncRNAs are  
49 dually classified as antisense (as) RNAs that are expressed from the same  
50 locus as a sense transcript in the opposite orientation. Current estimates  
51 using high-throughput transcriptome sequencing, indicate that up to 20-40%  
52 of the approximately 20,000 protein-coding genes exhibit antisense  
53 transcription (Chen et al. 2004, Katayama et al. 2005, Ozsolak et al. 2010).

54 Systematic large-scale studies have shown aberrant expression of asRNAs to  
55 be associated with tumorigenesis (Balbin et al. 2015) and, although  
56 characterization of several of these has identified asRNA-mediated regulation  
57 of multiple well known tumorigenic factors (Yap et al. 2010, Johnsson et al.  
58 2013), the vast majority of potential tumor-associated lncRNAs have not yet  
59 been characterized. The known mechanisms by which asRNAs accomplish  
60 their regulatory functions are diverse, and include recruitment of chromatin  
61 modifying factors (Rinn et al. 2007, Johnsson et al. 2013), acting as  
62 microRNA (miRNA) sponges (Memczak et al. 2013), and causing  
63 transcriptional interference (Conley et al. 2012).

64

65 Responses to cellular stress, e.g. DNA damage, sustained oncogene  
66 expression, and nutrient deprivation, are all tightly controlled cellular pathways  
67 that are almost universally dysregulated in cancer. Cellular signaling, in  
68 response to these types of stresses, often converges on the transcription  
69 factor TP53 that regulates transcription of coding and non-coding downstream  
70 targets. One important non-coding target of TP53 is the tumor suppressor  
71 microRNA known as *miR34a* (Raver-Shapira et al. 2007).  
72 Upon TP53 activation *miR34a* expression is increased allowing it to down-  
73 regulate target genes involved in cellular pathways such as growth factor  
74 signaling, apoptosis, differentiation, and cellular senescence (Lal et al. 2011,  
75 Slabakova et al. 2017). Thus, *miR34a* is a crucial factor in mediating activated  
76 TP53 response and, the fact that it is often deleted or down-regulated in  
77 human cancers both indicates, its tumor suppressive effect and makes it a  
78 valuable prognostic marker (Cole et al. 2008, Gallardo et al. 2009, Zenz et al.  
79 2009, Cheng et al. 2010, Liu et al. 2011). Reduced *miR34a* transcription is  
80 mediated via epigenetic regulation in many solid tumors, including colorectal-,  
81 pancreatic-, and ovarian cancer (Vogt et al. 2011), as well as numerous types  
82 of hematological malignancies (Chim et al. 2010). In addition, *miR34a* has  
83 been shown to be transcriptionally regulated via TP53 homologs, TP63 and  
84 TP73, other transcription factors, e.g. STAT3 and MYC, and, in addition, post-  
85 transcriptionally through miRNA sponging by the NEAT1 lncRNA (Chang et al.  
86 2008, Su et al. 2010, Agostini et al. 2011, Rokavec et al. 2015, Ding et al.  
87 2017). Despite these findings, the mechanisms underlying *miR34a* regulation  
88 in the context of oncogenesis have not yet been fully elucidated.

89

90 Studies across multiple cancer types have reported a decrease in oncogenic  
91 phenotypes when *miR34a* expression is induced in a *TP53*-null background,  
92 although endogenous mechanisms for achieving this have not yet been  
93 discovered (Liu et al. 2011, Ahn et al. 2012, Yang et al. 2012, Stahlhut et al.  
94 2015, Wang et al. 2015). In addition, previous reports from large-scale studies  
95 interrogating global *TP53*-mediated regulation of lncRNAs have identified a  
96 lncRNA (known as RP3-510D11.2 and LINC01759) originating in the  
97 antisense orientation from the *miR34a* locus which is induced upon numerous  
98 forms of cellular stress (Rashi-Elkeles et al. 2014, Hunten et al. 2015, Leveille  
99 et al. 2015, Ashouri et al. 2016, Kim et al. 2017). Despite this, none of these  
100 studies have functionally characterized this transcript. Therefore, in this study  
101 we functionally characterize the *miR34a* asRNA transcript, and find that it  
102 positively regulates *miR34a* expression resulting in a decrease of several  
103 tumorigenic phenotypes. Furthermore, we find that *miR34a* asRNA-mediated  
104 up-regulation of *miR34a* is sufficient to induce endogenous cellular  
105 mechanisms counteracting several types of stress stimuli in a *TP53*-deficient  
106 background. Finally, similar to the functional roles of antisense transcription at  
107 protein-coding genes, we identify a rare example of an antisense RNA  
108 capable of regulating a cancer-associated miRNA.

109

## 110 **Results**

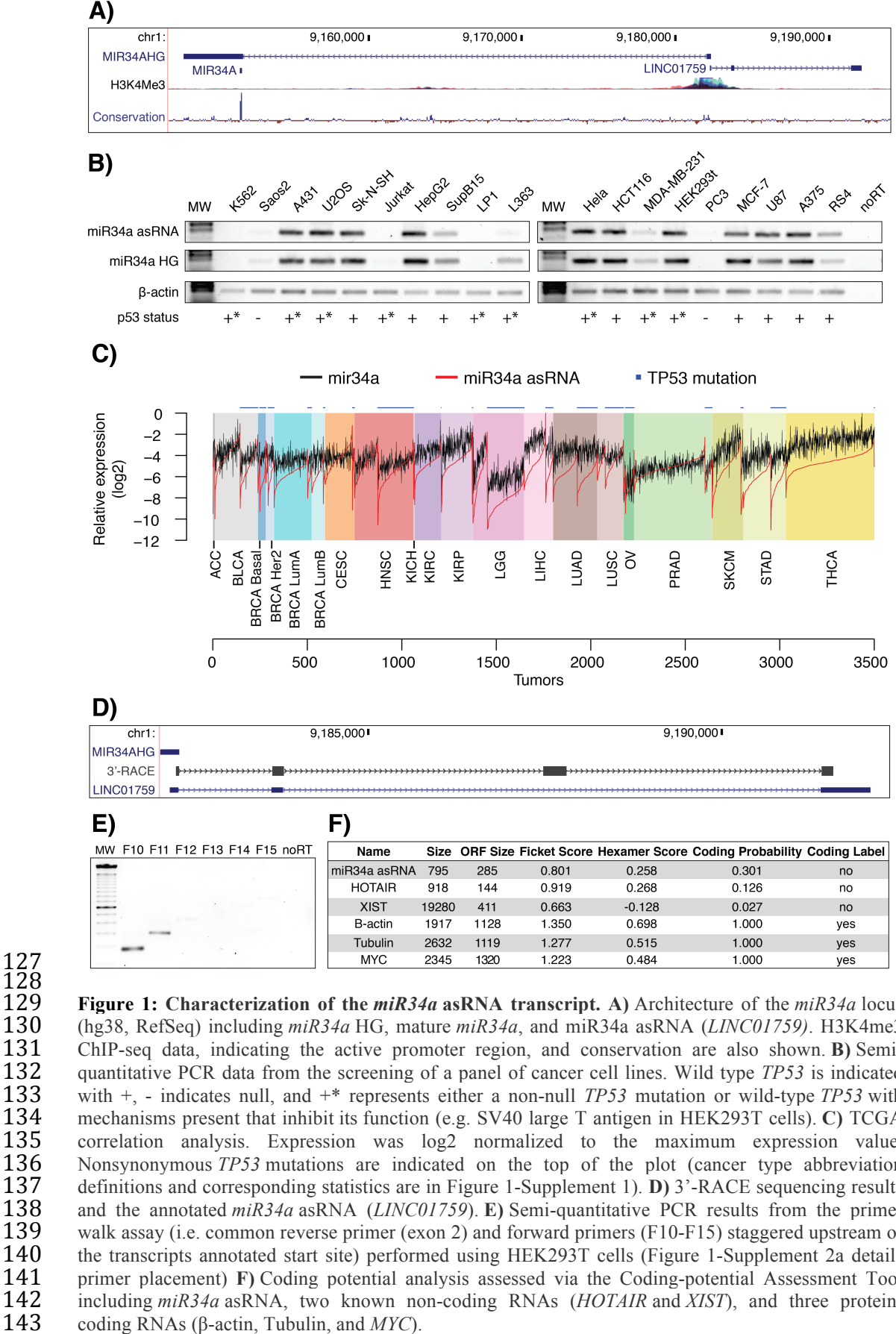
111

112 ***miR34a* asRNA is a broadly expressed, non-coding transcript whose**  
113 **levels correlate with *miR34a* expression**

114

115 *miR34a* asRNA is transcribed in a “head-to-head” orientation with  
116 approximately 100 base pair overlap with the *miR34a* host gene (HG) (**Fig.**  
117 **1a**). Due to the fact that sense/antisense pairs can be both concordantly and

118 discordantly expressed, we sought to evaluate this relationship in the case of  
119 *miR34a* HG and its asRNA. Using a diverse panel of cancer cell lines, we  
120 detected co-expression of both the *miR34a* HG and *miR34a* asRNA (**Fig. 1b**).  
121 We used cell lines with a known *TP53* status in the panel due to previous  
122 reports that *miR34a* is a known downstream target of TP53. These results  
123 indicate that *miR34a* HG and *miR34a* asRNA are co-expressed and that their  
124 expression levels correlate with *TP53* status, with *TP53*<sup>-/-</sup> cells tending to have  
125 decreased or undetectable expression of both transcripts.  
126



144 We next sought to analyze primary cancer samples to examine whether a  
145 correlation between *miR34a* asRNA and *miR34a* expression levels could be  
146 identified. We utilized RNA sequencing data from The Cancer Genome Atlas  
147 (TCGA) after stratifying patients by cancer type, *TP53* status, and, in the case  
148 of breast cancer, cancer subtypes. The results indicate that *miR34a* asRNA  
149 and *miR34a* expression are strongly correlated in the vast majority of cancer  
150 types examined, both in the presence and absence of wild-type *TP53* (**Fig.**  
151 **1c, Figure 1-Figure Supplement 1a**). The results also further confirm that  
152 the expression levels of both *miR34a* and its asRNA are significantly reduced  
153 in patients with nonsynonymous *TP53* mutations (**Figure 1-Figure**  
154 **Supplement 1b**).

155

156 Next, we aimed to gain a thorough understanding of *miR34a* asRNA's  
157 molecular characteristics and cellular localization. To experimentally  
158 determine the 3' termination site for the *miR34a* asRNA transcript we  
159 performed 3' rapid amplification of cDNA ends (RACE) using the U2OS  
160 osteosarcoma cell line that exhibited high endogenous levels  
161 of *miR34a* asRNA in the cell panel screening. Sequencing the cloned cDNA  
162 indicated that the transcripts 3' transcription termination site is 525 base pairs  
163 upstream of the *miR34a* asRNA transcript's annotated termination site (**Fig.**  
164 **1d**). Next, we characterized the *miR34a* asRNA 5' transcription start site by  
165 carrying out a primer walk assay, i.e. a common reverse primer was placed in  
166 exon 2 and forward primers were gradually staggered upstream of the  
167 transcripts annotated start site (**Figure 1-Figure Supplement 2a**). Our results  
168 indicated that the 5' start site for *miR34a* asRNA is in fact approximately 90bp

169 (F11 primer) to 220bp (F12 primer) upstream of the annotated start site (**Fig.**  
170 **1e**). Polyadenylation status was evaluated via cDNA synthesis with either  
171 random nanomers or oligo(DT) primers followed by semi-quantitative PCR  
172 which indicated that the *miR34a* asRNA is polyadenylated although the  
173 unspliced form seems to only be in a polyadenylation negative state (**Figure**  
174 **1-Figure Supplement 2b**). Furthermore, we investigated the propensity  
175 of *miR34a* asRNA to be alternatively spliced in U2OS cells, using PCR  
176 cloning followed by sequencing and found that the transcript is post-  
177 transcriptionally spliced to form multiple isoforms (**Figure 1-Figure**  
178 **Supplement 2c**). In order to evaluate the subcellular localization of *miR34a*  
179 asRNA, we made use of RNA sequencing data from five cancer cell lines  
180 included in the ENCODE (Consortium 2012) project that had been  
181 fractionated into cytosolic and nuclear fractions. The analysis revealed that  
182 the *miR34a* asRNA transcript primarily localizes to the nucleus with only a  
183 minor fraction in the cytosol (**Figure 1-Figure Supplement 2d**).

184  
185 Lastly, we utilized several approaches to evaluate the coding potential of  
186 the *miR34a* asRNA transcript. The Coding-Potential Assessment Tool is a  
187 bioinformatics-based tool that uses a logistic regression model to evaluate  
188 coding-potential by examining open reading frame (ORF) length, ORF  
189 coverage, Fickett score, and hexamer score (Wang et al. 2013). Results  
190 indicated that *miR34a* asRNA has a similar low coding capacity to known non-  
191 coding transcripts such as *HOTAIR* and *XIST* (**Fig. 1F**). We further confirmed  
192 these results using the Coding-Potential Calculator that uses a support vector  
193 machine-based classifier and accesses an alternate set of discriminatory

194 features (**Figure 1-Figure Supplement 2e**) (Kong et al. 2007). \*\*\* We hope to  
195 be able to scan for peptides matching to miR34a asRNA in CPTAC and  
196 Geiger et al., 2012 before submission and will mention results here.\*\*\*

197

198 **TP53-mediated regulation of *miR34a* asRNA expression**

199 *miR34a* is a known downstream target of TP53 and has been previously  
200 shown to exhibit increased expression within multiple contexts of cellular  
201 stress. *miR34a* asRNA has also been shown to be induced upon TP53  
202 activation in several global analyses of TP53-regulated lncRNAs (Rashi-  
203 Elkeles et al. 2014, Hunten et al. 2015, Leveille et al. 2015, Ashouri et al.  
204 2016, Kim et al. 2017). To confirm these results in our biological systems, we  
205 treated HEK293T, embryonic kidney cells, and HCT116, colorectal cancer  
206 cells, with the DNA damaging agent doxorubicin to activate TP53. QPCR-  
207 mediated measurements of both *miR34a* HG and asRNA indicated that their  
208 expression levels were increased in response to doxorubicin treatment in both  
209 cell lines (**Fig. 2a**). To assess whether TP53 was responsible for the increase  
210 in *miR34a* asRNA expression upon DNA damage, we  
211 treated *TP53*<sup>+/+</sup> and *TP53*<sup>-/-</sup> HCT116 cells with increasing concentrations of  
212 doxorubicin and monitored the expression of both *miR34a* HG and asRNA.  
213 We observed a dose-dependent increase in both *miR34a* HG and asRNA  
214 expression levels with increasing amounts of doxorubicin, indicating that  
215 these two transcripts are co-regulated, although, this effect was largely  
216 abrogated in *TP53*<sup>-/-</sup> cells (**Fig. 2b**). These results indicate  
217 that TP53 activation increases *miR34a* asRNA expression upon DNA  
218 damage. Nevertheless, *TP53*<sup>-/-</sup> cells also showed a dose-dependent increase

219 in both *miR34a* HG and asRNA, indicating that additional factors, other  
220 than *TP53* are capable of initiating an increase in expression of both of these  
221 transcripts upon DNA damage.

222

223  
224  
225  
226  
227  
228  
229  
230  
231  
232  
233  
234  
235  
236

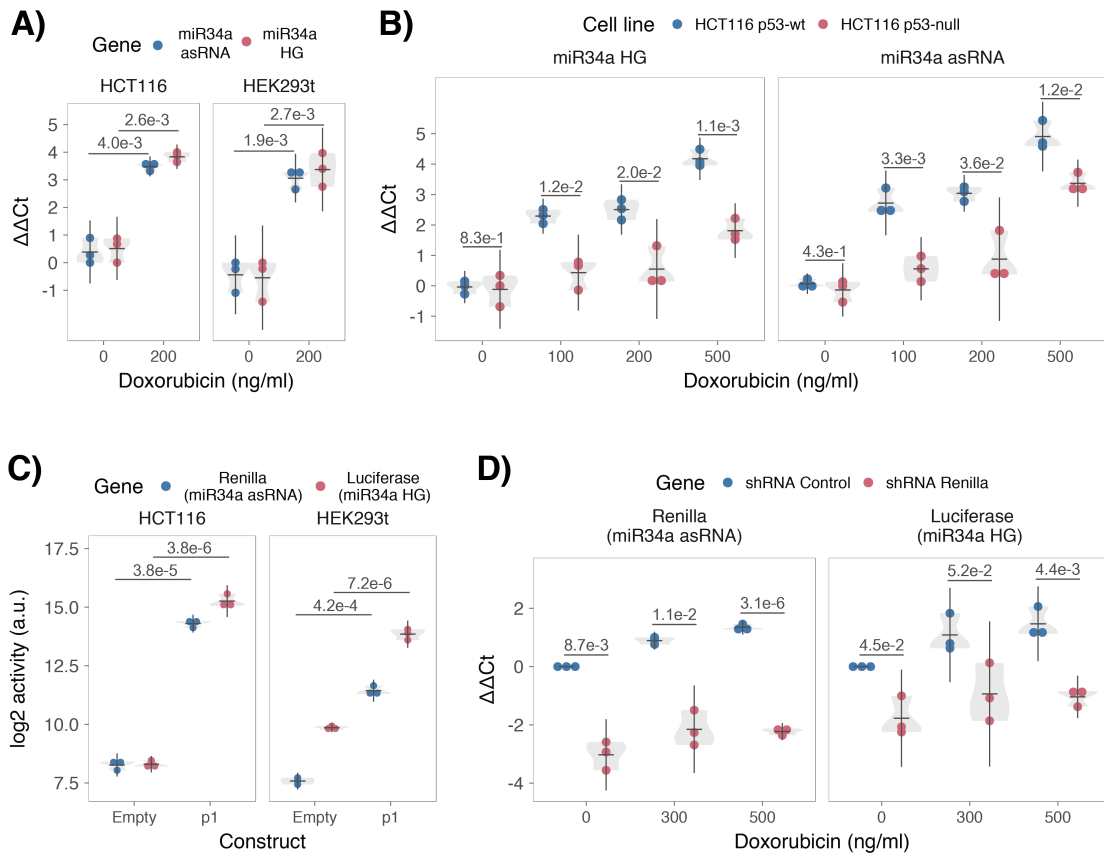


**Figure 2: TP53-mediated regulation of the *miR34a* locus.** **A)** Evaluating the effects of 24 hours of treatment with 200 ng/ml doxorubicin on *miR34a* asRNA and HG in HCT116 and HEK293T cells.\* **B)** Monitoring *miR34a* HG and asRNA expression levels during 24 hours of doxorubicin treatment in *TP53*<sup>+/+</sup> and *TP53*<sup>-/-</sup> HCT116 cells.\* **C)** Quantification of luciferase and renilla levels after transfection of HCT116 and HEK293T cells with the p1 construct (Figure 2-Supplement 2 contains a schematic representation of the p1 construct).\* **D)** HCT116 cells were co-transfected with the p1 construct and shRNA renilla or shRNA control and subsequently treated with increasing doses of doxorubicin. 24 hours post-treatment, cells were harvested and renilla and luciferase levels were measured using QPCR.\* Individual points represent results from independent experiments and the gray shadow indicates the density of those points. Error bars show the 95% CI, black horizontal lines represent the mean, and p-values are shown over long horizontal lines indicating the comparison tested. All experiments in Figure 2 were performed in biological triplicate.

237 The head-to-head orientation of *miR34a* HG and asRNA, suggests that  
238 transcription is initiated from a single promoter in a bi-directional manner (**Fig**  
239 **1a**). To investigate whether *miR34a* HG and asRNA are transcribed from the  
240 same promoter as divergent transcripts, we cloned the previously reported  
241 *miR34a* HG promoter, including the TP53 binding site, into a luciferase/renilla  
242 dual reporter vector which we hereafter refer to as p1 (**Figure 2-Figure**  
243 **Supplement 1a-b**) (Raver-Shapira et al. 2007). Upon transfection of p1 into  
244 HCT116 and HEK293T cell lines we observed increases in both luciferase  
245 and renilla indicating that *miR34a* HG and asRNA expression can be  
246 regulated by a single promoter contained within the p1 construct (**Fig. 2c**).  
247

248 ***miR34a* asRNA facilitates *miR34a* induction in response to DNA damage**  
249 We hypothesized that *miR34a* asRNA may regulate *miR34a* HG levels and, in  
250 addition, that the overlapping regions of the sense and antisense transcripts  
251 may mediate this regulation. Knockdown of endogenous *miR34a* asRNA is  
252 complicated by its various isoforms (**Figure 1-Figure Supplement 2c**). For  
253 this reason, we utilized the p1 construct to evaluate the regulatory role of the  
254 *miR34a* asRNA on *miR34a* HG. Accordingly, we first co-transfected the p1  
255 construct, containing the overlapping region of the two transcripts, and two  
256 different short hairpin (sh) RNAs targeting renilla into HEK293T cells and  
257 subsequently measured luciferase and renilla expression. The results  
258 indicated that shRNA-mediated knock down of the p1-renilla transcript  
259 (corresponding to *miR34a* asRNA) caused p1-luciferase (corresponding  
260 to *miR34a* HG) levels to concomitantly decrease (**Figure 2-Figure**  
261 **Supplement 2**). The results suggest that *miR34a* asRNA positively regulates

262 levels of *miR34a* HG and that the transcriptional product of the *miR34a*  
263 asRNA within in the p1 construct contributes to inducing a miR34a response.  
264 To further support these conclusions and better understand the role of  
265 *miR34a* asRNA during TP53 activation, *TP53<sup>+/+</sup>* HCT116 cells were co-  
266 transfected with p1 and shRNA renilla (2.1) and subsequently treated with  
267 increasing doses of doxorubicin. Again, the results showed a concomitant  
268 reduction in luciferase levels upon knock-down of p1-renilla i.e. the *miR34a*  
269 asRNA corresponding segment of the p1 transcript (**Fig. 2d**). Furthermore,  
270 the results showed that in the absence of p1-renilla the expected induction of  
271 p1-luciferase in response to TP53 activation by DNA damage is abrogated.  
272 Collectively these results indicate that *miR34a* asRNA positively regulates  
273 *miR34a* expression and furthermore, suggests that it is crucial for an  
274 appropriate TP53-mediated *miR34a* response to DNA damage.

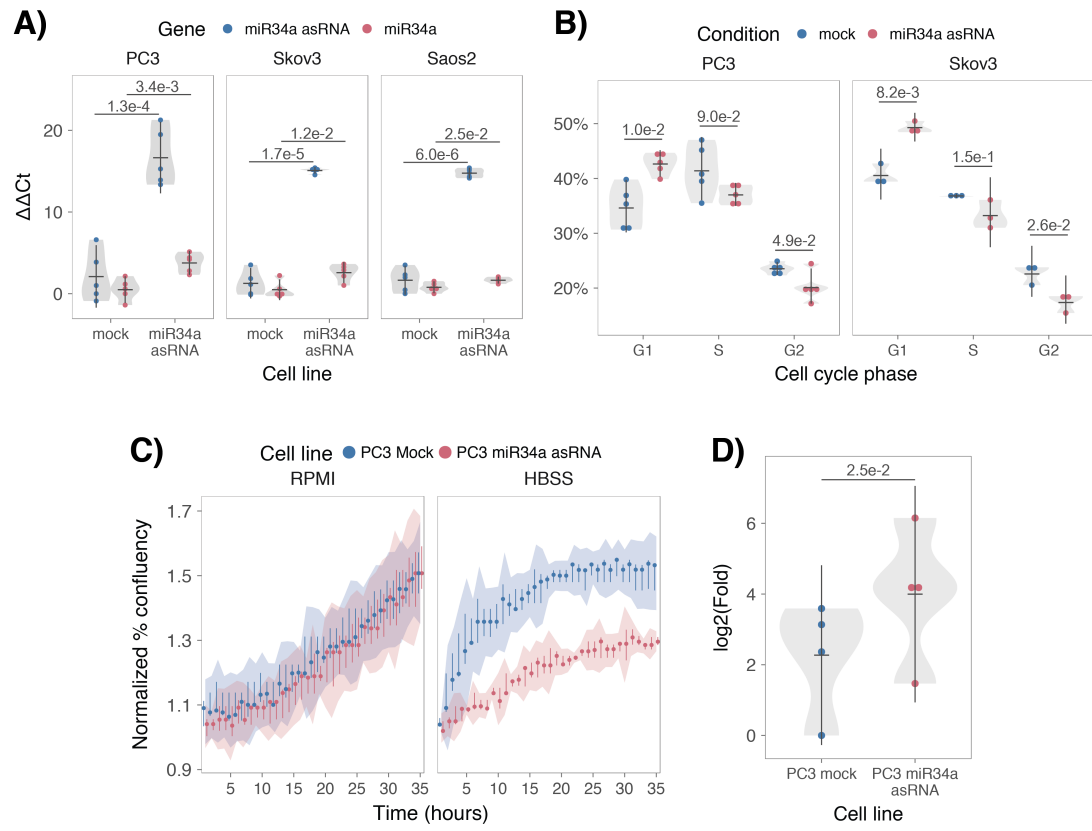
275

#### 276 ***miR34a* asRNA can regulate *miR34a* host gene independently of *TP53***

277 Despite the fact that TP53 regulates *miR34a* HG and asRNA expression, our  
278 results indicated that other factors are also able to regulate this locus (**Fig.**  
279 **2b**). Utilizing a lentiviral system, we stably over-expressed the *miR34a* asRNA  
280 transcript in three *TP53*-null cell lines, PC3 (prostate cancer), Saos2  
281 (osteogenic sarcoma), and Skov3 (ovarian adenocarcinoma). We first  
282 analyzed the levels of *miR34a* asRNA in these stable cell lines, compared to  
283 HEK293T cells, which have high endogenous levels of *miR34a* asRNA. On  
284 average, the over-expression was approximately 30-fold higher in the over-  
285 expression cell lines than in HEK293T cells, roughly corresponding to  
286 physiologically relevant levels in cells encountering a stress stimulus, such as

287 DNA damage (**Figure 3-Figure Supplement 1**). Analysis of *miR34a* levels in  
288 the *miR34a* asRNA over-expressing cell lines showed that this over-  
289 expression resulted in a concomitant increase in the expression of *miR34a* in  
290 all three cell lines (**Fig. 3a**). These results indicate that, in the absence of  
291 *TP53*, *miR34a* expression may be rescued by activating *miR34a* asRNA  
292 expression.

293



294 **Figure 3: miR34a asRNA positively regulates miR34a and its associated phenotypes.** **A)** QPCR-  
295 mediated quantification of miR34a expression in cell lines stably over-  
296 expressing miR34a asRNA.\* **B)** Cell cycle analysis comparing stably over-expressing miR34a asRNA  
297 cells to the respective mock expressing cells.\* **C)** Analysis of cellular growth over time in miR34a  
298 asRNA over-expressing PC3 cells. Points represent the median from 3 independent experiments, the  
299 colored shadows indicate the 95% confidence interval, and vertical lines show the minimum and  
300 maximum values obtained from the three experiments. **D)** Differential phosphorylated polymerase II  
301 binding in miR34a asRNA over-expressing PC3 cells.\* Individual points represent results from  
302 independent experiments and the gray shadow indicates the density of those points. Error bars show the  
303 95% CI, black horizontal lines represent the mean, and p-values are shown over long horizontal lines  
304 indicating the comparison tested.  
305

306 *miR34a* has been previously shown to regulate cell cycle progression, with  
307 *miR34a* induction causing G1 arrest (Raver-Shapira et al. 2007, Tarasov et al.  
308 2007). Cell cycle analysis via determination of DNA content showed a  
309 significant increase in G1 phase cells and a concomitant decrease in G2  
310 phase cells in the PC3 and Skov3 *miR34a* asRNA over-expressing cell lines,  
311 indicating G1 arrest (**Fig. 3b**). The effects of *miR34a* on the cell cycle are  
312 mediated by its ability to target cell cycle regulators such as cyclin D1  
313 (*CCND1*) (Sun et al. 2008). Quantification of both *CCND1* RNA expression  
314 (**Figure 3-Figure Supplement 2a**) and protein levels (**Figure 3-Figure**  
315 **Supplement 2b**) in the PC3 *miR34a* asRNA over-expressing cell line showed  
316 a significant decrease of *CCND1* levels compared to the mock control.  
317 Collectively, these results indicate that *miR34a* asRNA-mediated induction of  
318 *miR34a* is sufficient to result in the corresponding *miR34a*-directed effects on  
319 cell cycle.

320  
321 *miR34a* is also a well-known inhibitor of cellular growth via its ability to  
322 negatively regulate growth factor signaling. Furthermore, starvation has been  
323 shown to induce *miR34a* expression causing down-regulation of numerous  
324 pro-survival growth factors (Lal et al. 2011). We further interrogated the  
325 effects of *miR34a* asRNA over-expression by monitoring the growth of the  
326 PC3 stable cell lines in both normal and starvation conditions via confluency  
327 measurements over a 35-hour period. Under normal growth conditions there  
328 is a small but significant reduction ( $P = 3.0\text{e-}8$ ; linear regression, **Fig. 3c**) in  
329 confluency in the *miR34a* asRNA over-expressing cell lines compared to  
330 mock control. However, these effects on cell growth are drastically increased

331 in starvation conditions ( $P = 9.5\text{e-}67$ ; linear regression; **Fig. 3c**). This is in  
332 agreement with our previous results, and suggests that *miR34a* asRNA-  
333 mediated increases in *miR34a* expression are crucial under conditions of  
334 stress and necessary for the initiation of an appropriate cellular response. In  
335 summary, we find that over-expression of *miR34a* asRNA is sufficient to  
336 increase *miR34a* expression and gives rise to known phenotypes observed  
337 with induction of *miR34a*.

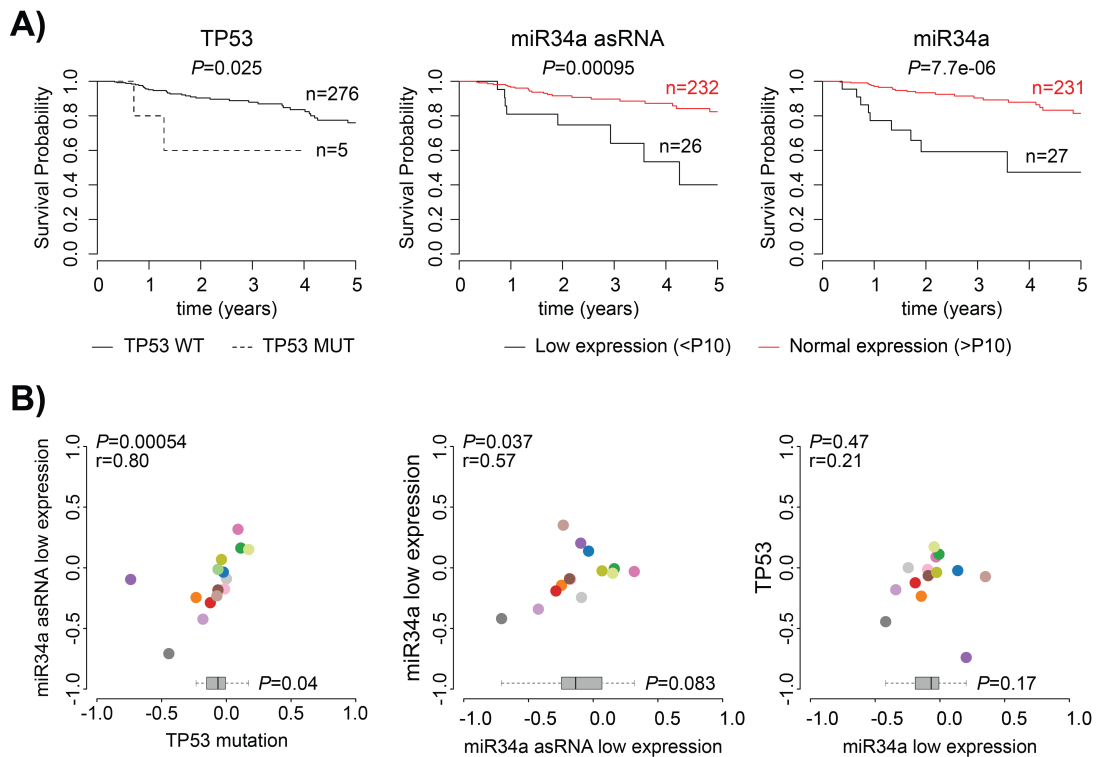
338

339 **miR34a asRNA transcriptionally activates miR34a host gene**

340 Antisense RNAs have been reported to mediate their effects both via  
341 transcriptional and post-transcriptional mechanisms. Due to the fact that  
342 *miR34a* expression is undetected in wild type PC3 cells (**Fig. 1b**) but, upon  
343 over-expression of *miR34a* asRNA, increases to detectable levels, we  
344 hypothesized that *miR34a* asRNA is capable of regulating *miR34a* expression  
345 via a transcriptional mechanism. To ascertain if this is actually the case, we  
346 performed chromatin immunoprecipitation (ChIP) for phosphorylated  
347 polymerase II (polII) at the *miR34a* HG promoter in both *miR34a* asRNA over-  
348 expressing and mock control cell lines. Our results indicated a clear increase  
349 in phosphorylated polII binding at the *miR34a* promoter upon *miR34a* asRNA  
350 over-expression indicating the ability of *miR34a* asRNA to regulate *miR34a*  
351 levels on a transcriptional level (**Fig. 3d**).

352

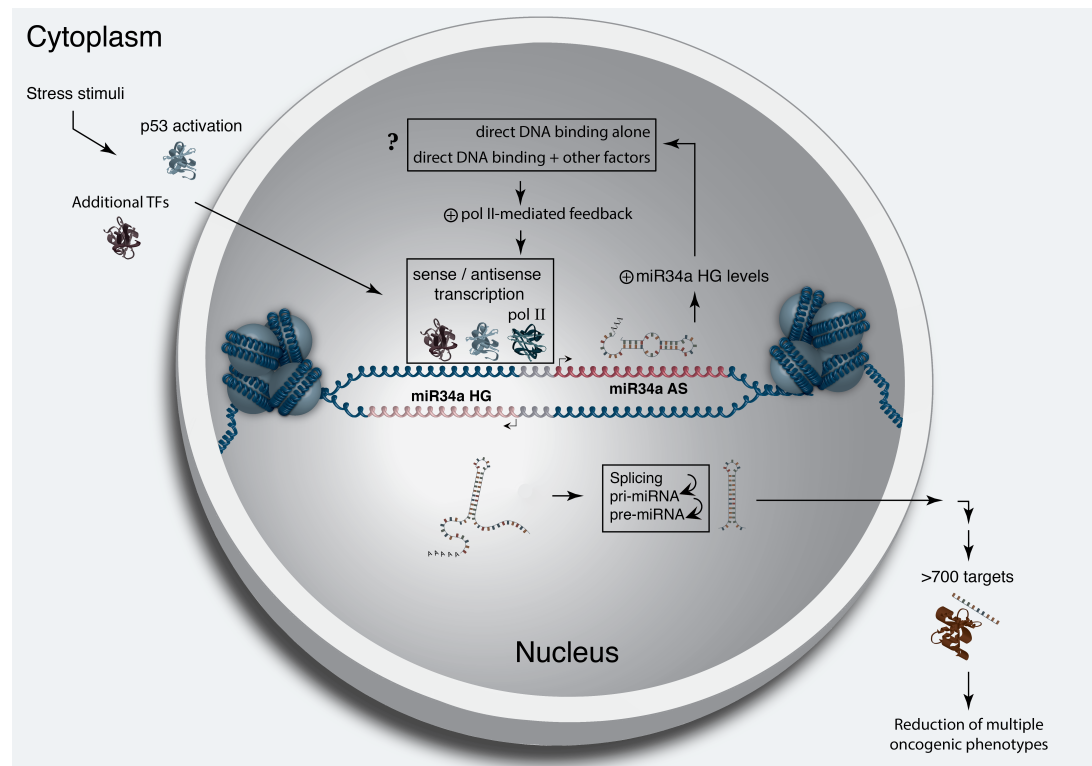
353



354 **Figure 4: Survival analysis.** A) Kaplan-Meier survival curves comparing the effects of TP53-mutated samples  
355 to control samples in papillary kidney cancer (results for other cancers in Figure 4-Supplement 1). B) Correlation  
356 analysis between the effects on the 5-year survival probability of TP53-mutated samples, low miR34a  
357 asRNA expression, and low miR34a expression as indicated. For each variable the 5-year survival  
358 probability was compared to the control group (negative value indicates lower survival, positive value  
359 indicates higher survival). Spearman correlation coefficients are given on top left of each plot. Each dot  
360 indicates one cancer type (see Fig.1c for legend). Boxplots on the bottom summarize the effects for the  
361 parameter on the x-axis, with indication of p-values, as calculated using paired Wilcoxon signed rank  
362 test. Low expression was defined as TP53 non-mutated samples having expression values in the bottom  
363 10th percentile.  
364

365  
366 **Low miR34a asRNA expression levels are associated with decreased**  
367 **survival**  
368  
369 As TP53 mutations and low expression of miR34a have been associated with  
370 worse prognosis in cancer, we compared survival rates of samples with low  
371 expression of miR34a asRNA (bottom 10th percentile) to control samples in  
372 17 cancer types from TCGA (**Figure 4-Supplement 1**) (Gallardo et al. 2009,  
373 Zenz et al. 2009, Liu et al. 2011). To correct for the effect of TP53 mutations  
374 we focused on non-TP53 mutated samples, and noted a worse survival for the  
375 low expression group in several cancers. This effect was most pronounced in  
376 papillary kidney cancer (unadjusted  $P=0.00095$ ; **Fig. 4a**). By systematically  
377 comparing 5-year survival probabilities between the low expression group and  
378 the control group for each cancer we found a median reduction of 5-year  
379 survival probability of 9.6% ( $P=0.083$ ; Wilcoxon signed rank test; **Fig. 4b**).  
380 Furthermore, we found that miR34a asRNA expression showed similar  
381 patterns in terms of direction and strength of association with 5-year survival  
382 probability as miR34a expression ( $r=0.57$ ,  $P=0.037$ ) and TP53 mutations  
383 ( $r=0.80$ ,  $P=0.00054$ ) across the different cancer types (**Fig. 4b**). Although  
384 these results do not implicate any causal relationship, they do indicate a  
385 striking similarity between the association of worse prognosis and TP53  
386 mutations, low miR34a, and low miR34a asRNA expression.

387



388

**Figure 5: A graphical summary of the proposed *miR34a* asRNA function.** Stress stimuli, originating in the cytoplasm or nucleus, activate TP53 as well as additional factors. These factors then bind to the *miR34a* promoter and drive transcription of the sense and antisense strands. *miR34a* asRNA serves to further increase the levels of *miR34a* HG transcription resulting in enrichment of polymerase II at the *miR34a* promoter and a positive feed-forward loop. *miR34a* asRNA-mediated increases in *miR34a* HG potentially occur via direct DNA binding alone, by direct DNA binding and recruitment of additional factors, or through a yet unknown mechanism. *miR34a* HG then, in turn, is spliced and processed before being exported to the cytoplasm. The *miR34a* pre-miRNA then undergoes further processing before the mature *miR34a* binds to the RISC complex allowing it to bind and repress its targets and exert its tumor suppressive effects.

398 **Discussion**

399  
400 Multiple studies have previously shown asRNAs to be crucial for the  
401 appropriate regulation of cancer-associated protein-coding genes and that  
402 their dysregulation can lead to a perturbation of tumor suppressive and  
403 oncogenic pathways, as well as, cancer-related phenotypes (Yu et al. 2008,  
404 Yap et al. 2010, Serviss et al. 2014, Balbin et al. 2015). Here we show that  
405 asRNAs are also capable of regulating cancer-associated miRNAs resulting in  
406 similar consequences as protein-coding gene dysregulation (**Fig. 4**).  
407 Interestingly, we show that, both in the presence and absence of  
408 *TP53*, *miR34a* asRNA provides an additional regulatory level to control  
409 *miR34a* expression in both homeostasis and upon encountering various forms  
410 of cellular stress. Furthermore, we find that a *miR34a* asRNA-mediated  
411 increase in *miR34a* expression is sufficient to drive the appropriate cellular  
412 responses to these stress stimuli (**Fig. 2d and Fig. 3c**). Previous studies have  
413 exploited various molecular biology methods to up-regulate *miR34a*  
414 expression in a *TP53*-deficient background showing similar phenotypic  
415 outcomes although, here we show a novel mechanism by which this can be  
416 achieved in an endogenous manner (Liu et al. 2011, Ahn et al. 2012, Yang et  
417 al. 2012, Stahlhut et al. 2015, Wang et al. 2015).

418

419 In agreement with previous studies, we demonstrate that upon encountering  
420 various types of cellular stress, *TP53* in concert with additional factors bind  
421 and initiate transcription at the *miR34a* locus, thus increasing the levels of  
422 *miR34a* asRNA and, in addition, *miR34a*. We found that overexpression of  
423 *miR34a* asRNA leads to recruitment of polymerase II to the *miR34a* promoter

424 and hypothesize that *miR34a* asRNA may provide positive feedback for  
425 *miR34a* expression whereby it serves as a scaffold for the recruitment of  
426 additional factors that facilitate polymerase II-mediated transcription. In this  
427 manner, *miR34a* expression is induced and thus, drives a shift towards a  
428 reduction in growth factor signaling, senescence, and in some cases  
429 apoptosis. On the other hand, in cells without functional TP53, other factors,  
430 which typically act independently or in concert with TP53, may initiate  
431 transcription of the *miR34a* locus. In this scenario *miR34a* asRNA could  
432 potentially be interacting directly with one of these additional factors and  
433 recruiting it to the *miR34a* locus in order to drive *miR34a* transcription. The  
434 head-to-head orientation of the *miR34a* HG and asRNA causes sequence  
435 complementarity between the RNA and the promoter DNA, making this an  
436 attractive mechanism. Previous reports have also illustrated the ability of  
437 asRNAs to form hybrid DNA:RNA R-loops and, thus, facilitate an open  
438 chromatin structure and the transcription of the sense gene (Boque-Sastre et  
439 al. 2015). The fact that the p1 construct only contains a small portion (307 bp)  
440 of the *miR34a* asRNA transcript indicates that this portion is sufficient to give  
441 rise to at least a partial *miR34a* inducing response and therefore, that *miR34a*  
442 asRNA may be able to facilitate *miR34a* expression independent of additional  
443 factors (**Fig 2d, Figure 2-Figure Supplement 2a**). Nevertheless, further work  
444 will need to be performed to explore the mechanism whereby *miR34a* asRNA  
445 regulates *miR34a* gene expression.

446

447 An antisense transcript arising from the *miR34a* locus, *Lnc34a*, has been  
448 previously reported to negatively regulate the expression of *miR34a* (Wang et

449 al. 2016). Although the *Lnc34a* and *miR34a* asRNA transcripts share some  
450 sequence similarity, we believe them to be separate RNAs that are,  
451 potentially, different isoforms of the same gene. We utilized CAGE and  
452 RNAseq data from the ENCODE project to evaluate the presence of *miR34a*  
453 asRNA and *Lnc34a* in 28 and 36 commonly used cancer cell lines,  
454 respectively. Although the results show the presence of *miR34a* asRNA in  
455 these cell lines, we find no evidence for *Lnc34a* transcription (**Supplementary**  
456 **Document 1**). These results are in line with the findings of Wang et al.  
457 indicating that *Lnc34a* is highly expressed in colon cancer stem cell spheres  
458 compared to other cell types used in their study and, furthermore suggests,  
459 that these two transcripts are not commonly co-expressed. The fact  
460 that *Lnc34a* and *miR34a* asRNA would appear to have opposing roles in their  
461 regulation of *miR34a* further underlines the complexity of the regulation at this  
462 locus.

463

464 Clinical trials utilizing miR34a replacement therapy have previously been  
465 conducted but, disappointingly, were terminated after adverse side effects of  
466 an immunological nature were observed in several of the patients (Slabakova  
467 et al. 2017). Although it is not presently clear if these side effects were caused  
468 by *miR34a* or the liposomal carrier used to deliver the miRNA, the multitude of  
469 evidence indicating *miR34a*'s crucial role in oncogenesis still makes its  
470 therapeutic induction an interesting strategy and needs further investigation.  
471 Our results indicate a association between survival probability and low  
472 *miR34a* asRNA expression making it an attractive candidate for controlled  
473 preclinical studies. Due to *miR34a* asRNA-mediated positive feedback on

474 *miR34a* expression, initiation of this feedback mechanism may be able to  
475 provide a sustained *miR34a* induction in a relatively more robust manner than  
476 *miR34a* replacement alone. In summary, our results have identified *miR34a*  
477 asRNA as a vital player in the regulation of *miR34a* and its particular  
478 importance in typical examples of cellular stress encountered in cancer. The  
479 conclusions drawn in this study provide essential insight regarding asRNA-  
480 mediated regulation of cancer-associated miRNAs and, contribute to  
481 fundamental knowledge concerning *miR34a* regulation necessary for its  
482 efficient induction in clinical settings.

483

## 484 **Materials and Methods**

### 485 **Cell Culture**

486 All cell lines were cultured at 5% CO<sub>2</sub> and 37°C with HEK293T, Saos2, and  
487 Skov3 cells cultured in DMEM high glucose (GE Healthcare Life Sciences,  
488 Hyclone, Amersham. UK, Cat# SH30081), HCT116 and U2OS cells in  
489 McCoy's 5a (ThermoFisher Scientific, Pittsburgh, MA, USA. Cat# SH30200),  
490 and PC3 cells in RPMI (GE Healthcare Life Sciences, Hyclone, Cat#  
491 SH3009602) and 2 mM L-glutamine (GE Healthcare Life Sciences, Hyclone,  
492 Cat# SH3003402). All growth mediums were supplemented with 10% heat-  
493 inactivated FBS (ThermoFisher Scientific, Gibco, Cat# 12657029) and 50  
494 µg/ml of streptomycin (ThermoFisher Scientific, Gibco, Cat# 15140122) and  
495 50 µg/ml of penicillin (ThermoFisher Scientific, Gibco, Cat# 15140122). All cell  
496 lines were purchased from ATCC, tested negative for mycoplasma, and their  
497 identity was verified via STR profiling.

498

### 499 **Bioinformatics, Data Availability, and Statistical Testing**

500 The USCS genome browser (Kent et al. 2002) was utilized for the  
501 bioinformatic evaluation of antisense transcription utilizing the RefSeq  
502 (O'Leary et al. 2016) gene annotation track.

503

504 All raw experimental data, code used for analysis, and supplementary  
505 methods are available for review at ([Serviss 2017](#)) and are provided as an R  
506 package. All analysis took place using the R statistical programming language  
507 (Team 2017) using external packages that are documented in the package  
508 associated with this article (Wilkins , Chang 2014, Wickham 2014, Therneau  
509 2015, Wickham 2016, Allaire et al. 2017, Arnold 2017, Wickham 2017,  
510 Wickham 2017, Wickham 2017, Xiao 2017, Xie 2017). The package facilitates  
511 replication of the operating system and package versions used for the original  
512 analysis, reproduction of each individual figure and figure supplement  
513 included in the article, and easy review of the code used for all steps of the  
514 analysis, from raw-data to figure.

515

516 The significance threshold (alpha) in this study was set to 0.05. Statistical  
517 testing was performed using a unpaired two sample Student's t-test unless  
518 otherwise specified.

519

## 520 **Coding Potential**

521 Protein-coding capacity was evaluated using the Coding-potential  
522 Assessment Tool (Wang et al. 2013) and Coding-potential Calculator (Kong et  
523 al. 2007) with default settings. Transcript sequences for use with Coding-  
524 potential Assessment Tool were downloaded from the UCSC genome

525 browser using the Ensembl  
526 accessions: *HOTAIR* (ENST00000455246), *XIST* (ENST00000429829), β-  
527 actin (ENST00000331789), Tubulin (ENST00000427480),  
528 and *MYC* (ENST00000377970). Transcript sequences for use with Coding-  
529 potential Calculator were downloaded from the UCSC genome browser using  
530 the following IDs: *HOTAIR* (uc031qho.1), β-actin (uc003soq.4).

531

### 532 **shRNAs**

533 shRNA-expressing constructs were cloned into the U6M2 construct using the  
534 BgIII and KpnI restriction sites as previously described (Amarzguioui et al.  
535 2005). shRNA constructs were transfected using Lipofectamine 2000 or 3000  
536 (ThermoFisher Scientific, Cat# 12566014 and L3000015). The sequences  
537 targeting renilla is as follows: shRenilla 1.1 (AAT ACA CCG CGC TAC TGG  
538 C), shRenilla 2.1 (TAA CGG GAT TTC ACG AGG C).

539

### 540 **Bi-directional Promoter Cloning**

541 The overlapping region (p1) corresponds with the sequence previously  
542 published as the TP53 binding site in (Raver-Shapira et al. 2007) which we  
543 synthesized, cloned into the pLucRluc construct (Polson et al. 2011) and  
544 sequenced to verify its identity.

545

### 546 **Promoter Activity**

547 Cells were co-transfected with the renilla/firefly bidirectional promoter  
548 construct (Polson et al. 2011) and GFP by using Lipofectamine 2000 (Life  
549 Technologies, Cat# 12566014). The expression of GFP and luminescence

550 was measured 24 h post transfection by using the Dual-Glo Luciferase Assay  
551 System (Promega, Cat# E2920) and detected by the GloMax-Multi+ Detection  
552 System (Promega, Cat# SA3030). The expression of luminescence was  
553 normalized to GFP.

554

555 **Generation of U6-expressed miR34a AS Lentiviral Constructs**

556 The U6 promoter was amplified from the U6M2 cloning plasmid (Amarzguioui  
557 et al. 2005) and ligated into the Not1 restriction site of the pHIV7-IMPDH2  
558 vector (Turner et al. 2012). *miR43a* asRNA was PCR amplified and  
559 subsequently cloned into the Nhe1 and Pac1 restriction sites in the pHIV7-  
560 IMPDH2-U6 plasmid.

561

562 **Lentiviral Particle production, infection, and selection**

563 Lentivirus production was performed as previously described in (Turner et al.  
564 2012). Briefly, HEK293T cells were transfected with viral and expression  
565 constructs using Lipofectamine 2000 (ThermoFisher Scientific, Cat#  
566 12566014), after which viral supernatants were harvested 48 and 72 hours  
567 post-transfection. Viral particles were concentrated using PEG-IT solution  
568 (Systems Biosciences, Palo Alto, CA, USA. Cat# LV825A-1) according to the  
569 manufacturer's recommendations. HEK293T cells were used for virus titration  
570 and GFP expression was evaluated 72hrs post-infection via flow cytometry  
571 (LSRII, BD Biosciences, San Jose, CA, USA) after which TU/ml was  
572 calculated.

573

574 Stable lines were generated by infecting cells with a multiplicity of infection of

575 1 after which 1-2 µM mycophenolic acid (Merck, Kenilworth, NJ, USA. Cat#  
576 M5255) selection was initiated 48 hours post-infection. Cells were expanded  
577 as the selection process was monitored via flow cytometry analysis (LSRII,  
578 BD Biosciences) of GFP and selection was terminated once > 90% of the  
579 cells were GFP positive. Quantification of *miR34a* asRNA over-expression  
580 and *miR34a* was performed in biological quintuplet for all cell lines.

581

### 582 **Western Blotting**

583 Samples were lysed in 50 mM Tris-HCl (Sigma Aldrich, St. Louis, MO, USA.  
584 Cat# T2663), pH 7.4, 1% NP-40 (Sigma Aldrich, Cat# I8896), 150 mM NaCl  
585 (Sigma Aldrich, Cat# S5886), 1 mM EDTA (Promega, Madison, WI, USA.  
586 Cat# V4231), 1% glycerol (Sigma Aldrich, Cat# G5516), 100 µM vanadate  
587 (Sigma Aldrich, Cat# S6508), protease inhibitor cocktail (Roche Diagnostics,  
588 Basel, Switzerland, Cat# 004693159001) and PhosSTOP (Roche  
589 Diagnostics, Cat# 04906837001). Lysates were subjected to SDS-PAGE and  
590 transferred to PVDF membranes. The proteins were detected by western blot  
591 analysis by using an enhanced chemiluminescence system (Western  
592 Lightning-ECL, PerkinElmer, Waltham, MA, USA. Cat# NEL103001EA).  
593 Antibodies used were specific for CCND1 1:1000 (Cell Signaling, Danvers,  
594 MA, USA. Cat# 2926), and GAPDH 1:5000 (Abcam, Cambridge, UK, Cat#  
595 ab9485). All western blot quantifications were performed using ImageJ  
596 (Schneider et al. 2012).

597

### 598 **RNA Extraction and cDNA Synthesis**

599 For downstream SYBR green applications, RNA was extracted using the

600 RNeasy mini kit (Qiagen, Venlo, Netherlands, Cat# 74106) and subsequently  
601 treated with DNase (Ambion Turbo DNA-free, ThermoFisher Scientific, Cat#  
602 AM1907). 500ng RNA was used for cDNA synthesis using MuMLV  
603 (ThermoFisher Scientific, Cat# 28025013) and a 1:1 mix of oligo(dT) and  
604 random nanomers.

605

606 For analysis of miRNA expression with Taqman, samples were isolated with  
607 TRIzol reagent (ThermoFisher Scientific, Cat# 15596018) and further  
608 processed with the miRNeasy kit (Qiagen, Cat# 74106). cDNA synthesis was  
609 performed using the TaqMan MicroRNA Reverse Transcription Kit  
610 (ThermoFisher Scientific, Cat# 4366597) using the corresponding oligos  
611 according to the manufacturer's recommendations.

612

### 613 QPCR and PCR

614 PCR was performed using the KAPA2G Fast HotStart ReadyMix PCR Kit  
615 (Kapa Biosystems, Wilmington, MA, USA, Cat# KK5601) with corresponding  
616 primers. QPCR was carried out using KAPA 2G SYBRGreen (Kapa  
617 Biosystems, Cat# KK4602) using the Applied Biosystems 7900HT machine  
618 with the cycling conditions: 95 °C for 3 min, 95 °C for 3 s, 60 °C for 30 s.

619

620 QPCR for miRNA expression analysis was performed according to the primer  
621 probe set manufacturers recommendations (ThermoFisher Scientific) and  
622 using the TaqMan Universal PCR Master Mix (ThermoFisher Scientific, Cat#  
623 4304437) with the same cycling scheme as above. Primer and probe sets for  
624 TaqMan were also purchased from ThermoFisher Scientific (Life

625 Technologies at time of purchase, TaqMan® MicroRNA Assay, hsa-miR-34a,  
626 human, Cat# 4440887, Assay ID: 000426 and Control miRNA Assay, RNU48,  
627 human, Cat# 4440887, Assay ID: 001006).

628

629 The  $\Delta\Delta Ct$  method was used to quantify gene expression. All QPCR-based  
630 experiments were performed in at least technical duplicate. Primers for all  
631 PCR-based experiments are listed in **Supplementary Document 2** and  
632 arranged by figure.

633

#### 634 **Cell Cycle Distribution**

635 Cells were washed in PBS and fixed in 4% paraformaldehyde at room  
636 temperature overnight. Paraformaldehyde was removed, and cells were re-  
637 suspended in 95% EtOH. The samples were then rehydrated in distilled  
638 water, stained with DAPI and analyzed by flow cytometry on a LSRII (BD  
639 Biosciences) machine. Resulting cell cycle phases were quantified using the  
640 ModFit software (Verity Software House, Topsham, ME, USA). Experiments  
641 were performed in biological quadruplet (PC3) or triplicate (Skov3). The log2  
642 fraction of cell cycle phase was calculated for each replicate a two sample t-  
643 test was utilized for statistical testing.

644

#### 645 **3' Rapid Amplification of cDNA Ends**

646 3'-RACE was performed as described as previously in (Johnsson et al. 2013).  
647 Briefly, U2OS cell RNA was polyA-tailed using yeast polyA polymerase  
648 (ThermoFisher Scientific, Cat# 74225Z25KU) after which cDNA was  
649 synthesized using oligo(dT) primers. Nested-PCR was performed first using a

650 forward primer in *miR34a* asRNA exon 1 and a tailed oligo(dT) primer  
651 followed by a second PCR using an alternate *miR34a* asRNA exon 1 primer  
652 and a reverse primer binding to the tail of the previously used oligo(dT)  
653 primer. PCR products were gel purified and cloned the Strata Clone Kit  
654 (Agilent Technologies, Santa Clara, CA, USA. Cat# 240205), and sequenced.

655

### 656 **Chromatin Immunoprecipitation**

657 The ChIP was performed as previously described in (Johnsson et al. 2013)  
658 with the following modifications. Cells were crosslinked in 1% formaldehyde  
659 (Merck, Cat# 1040039025), quenched with 0.125M glycine (Sigma Aldrich,  
660 Cat# G7126), and lysed in cell lysis buffer comprised of: 5mM PIPES (Sigma  
661 Aldrich, Cat# 80635), 85mM KCL (Merck, Cat# 4936), 0.5% NP40 (Sigma  
662 Aldrich, Cat# I8896), protease inhibitor (Roche Diagnostics, Cat#  
663 004693159001). Samples were then sonicated in 50mM TRIS-HCL pH 8.0  
664 (Sigma Aldrich, MO, USA, Cat# T2663) 10mM EDTA (Promega, WI, USA,  
665 Cat# V4231), 1% SDS (ThermoFisher Scientific, Cat# AM9822), and protease  
666 inhibitor (Roche Diagnostics, Cat# 004693159001) using a Bioruptor  
667 Sonicator (Diagenode, Denville, NJ, USA). Samples were incubated over  
668 night at 4°C with the polII antibody (Abcam, Cat# ab5095) and subsequently  
669 pulled down with Salmon Sperm DNA/Protein A Agarose (Millipore, Cat# 16-  
670 157) beads. DNA was eluted in an elution buffer of 1% SDS (ThermoFisher  
671 Scientific, Cat# AM9822) 100mM NaHCO3 (Sigma Aldrich, Cat# 71631),  
672 followed by reverse crosslinking, RNaseA (ThermoFisher Scientific, Cat#  
673 1692412) and protease K (New England Biolabs, Ipswich, MA, USA, Cat#  
674 P8107S) treatment. The DNA was eluted using Qiagen PCR purification kit

675 (Cat# 28106) and quantified via QPCR. QPCR was performed in technical  
676 duplicate using the standard curve method and reported absolute values. The  
677 fraction of input was subsequently calculated using the mean of the technical  
678 replicates followed by calculating the fold over the control condition. Statistical  
679 testing was performed using 4 biological replicates with the null hypothesis  
680 that the true log 2 fold change values were equal to zero.

681

## 682 **Confluency Analysis**

683 Cells were incubated in the Spark Multimode Microplate (Tecan, Männedorf,  
684 Switzerland) reader for 48 hours at 37°C with 5% CO<sub>2</sub> in a humidity chamber.  
685 Confluency was measured every hour using bright-field microscopy and the  
686 percentage of confluency was reported via the plate reader's inbuilt algorithm.  
687 Percentage of confluency was normalized to the control sample in each  
688 condition (shown in figure) and then ranked to move the data to a linear scale.  
689 Using the mean of the technical duplicates in three biological replicates, the  
690 rank was then used to construct a linear model, of the dependency of the rank  
691 on the time and cell lines variables for each growth condition. Reported p-  
692 values are derived from the t-test, testing the null hypothesis that the  
693 coefficient estimate of the cell line variable is equal to 0.

694

## 695 **Pharmacological Compounds**

696 Doxorubicin was purchased from Teva (Petah Tikva, Israel, cat. nr. 021361).

697

## 698 **Cellular Localization Analysis**

699 Quantified RNAseq data from 11 cell lines from the GRCh38 assembly was

700 downloaded from the ENCODE project database and quantifications for  
701 *miR34a* asRNA (ENSG00000234546), GAPDH (ENSG00000111640), and  
702 MALAT1 (ENSG00000251562) were extracted. Cell lines for which data was  
703 downloaded include: A549, GM12878, HeLa-S3, HepG2, HT1080, K562  
704 MCF-7, NCI-H460, SK-MEL-5, SK-N-DZ, SK-N-SH. Initial exploratory analysis  
705 revealed that several cell lines should be removed from the analysis due to a)  
706 a larger proportion of GAPDH in the nucleus than cytoplasm or b) variation of  
707 *miR34a* asRNA expression is too large to draw conclusions, or c) they have  
708 no or low (<6 TPM) *miR34a* asRNA expression. Furthermore, only  
709 polyadenylated libraries were used in the final analysis, due to the fact that  
710 the cellular compartment enrichment was improved in these samples. All  
711 analyzed genes are reported to be polyadenylated. In addition, only samples  
712 with 2 biological replicates were retained. For each cell type, gene, and  
713 biological replicate the fraction of transcripts per million (TPM) in each cellular  
714 compartment was calculated as the fraction of TPM in the specific  
715 compartment by the total TPM. The mean and standard deviation for the  
716 fraction was subsequently calculated for each cell type and cellular  
717 compartment and this information was represented in the final figure.

718

## 719 **CAGE Analysis**

720 All available CAGE data from the ENCODE project (Consortium 2012) for 36  
721 cell lines was downloaded from the UCSC genome browser (Kent et al. 2002)  
722 for genome version hg19. Of these, 28 cell lines had CAGE transcription start  
723 sites (TSS) mapping to the plus strand of chromosome 1 and in regions  
724 corresponding to 200 base pairs upstream of the *lnc34a* start site (9241796 -

725 200) and 200 base pairs upstream of the GENCODE  
726 annotated *miR34a* asRNA start site (9242263 + 200). These cell lines  
727 included: HFDPC, H1-hESC, HMEpC, HAoEC, HPIEpC, HSaVEC, GM12878,  
728 hMSC-BM, HUVEC, AG04450, hMSC-UC, IMR90, NHDF, SK-N-SH\_RA, BJ,  
729 HOB, HPC-PL, HAoAF, NHEK, HVMF, HWP, MCF-7, HepG2, hMSC-AT,  
730 NHEM.f\_M2, SkMC, NHEM\_M2, and HCH. In total 74 samples were included.  
731 17 samples were polyA-, 47 samples were polyA+, and 10 samples were total  
732 RNA. In addition, 34 samples were whole cell, 15 enriched for the cytosolic  
733 fraction, 15 enriched for the nucleolus, and 15 enriched for the nucleus. All  
734 CAGE transcription start sites were plotted and the RPKM of the individual  
735 reads was used to color each read to indicate their relative abundance. In  
736 cases where CAGE TSS spanned identical regions, the RPMKs of the regions  
737 were summed and represented as one CAGE TSS in the figure. In addition, a  
738 density plot shows the distribution of the CAGE reads in the specified  
739 interval.

740

#### 741 **Splice Junction Analysis**

742 All available whole cell (i.e. non-fractionated) spliced read data originating  
743 from the Cold Spring Harbor Lab in the ENCODE project (Consortium 2012)  
744 for 38 cell lines was downloaded from the UCSC genome browser (Kent et al.  
745 2002). Of these cell lines, 36 had spliced reads mapping to the plus strand of  
746 chromosome 1 and in the region between the *lnc34a* start (9241796) and  
747 transcription termination (9257102) site (note that *miR34a* asRNA resides  
748 totally within this region). Splice junctions from the following cell lines were  
749 included in the final figure: A549, Ag04450, Bj, CD20, CD34 mobilized,

750 Gm12878, H1hesc, Haoaf, Haoec, Hch, Helas3, Hepg2, Hfdpc, Hmec,  
751 Hmepc, Hmscat, Hmscbm, Hmscuc, Hob, Hpcpl, Hpiepc, Hsavec, Hsmm,  
752 Huvec, Hvmf, Hwp, Imr90, Mcf7, Monocd14, Nhdf, Nhek, Nhjemfm2,  
753 Nhemm2, Nhlf, Skmc, and Sknsh. All splice junctions were included in the  
754 figure and colored according to the number of reads corresponding to each. In  
755 cases where identical reads were detected multiple times, the read count was  
756 summed and represented as one read in the figure.

757

## 758 **TCGA Data Analysis**

759 RNA-Seq data and copy number data were downloaded from TCGA and  
760 processed as described previously (Ashouri et al. 2016). Briefly, RNA-Seq  
761 data were aligned to the human hg19 assembly and quantified using  
762 GENCODE (v19) annotated HTSeq-counts and FPKM normalizations.  
763 Expression data from miR34a and miR34 asRNA (identified as RP3-  
764 510D11.2) were used for further analysis. Copy number amplitudes for  
765 GENCODE genes were determined from segmented copy-number data.  
766 Samples that were diploid for miR34 asRNA were identified as those samples  
767 that had copy number amplitudes between -0.1 and 0.1.

768

769 Somatic mutation data were downloaded from the Genomics Data Commons  
770 data portal (GDC) as mutation annotation format (maf) files, called using  
771 Mutect2 on 30/10/2017 (v7) (Grossman et al. 2016).

772

773 Survival analysis was performed on TCGA vital state and follow-up data,  
774 downloaded from GDC on 27/10/2017 using the R survival package  
775 (Therneau 2015).

776

777 **Acknowledgments**

778 The authors would like to kindly thank Martin Enge for his critical review of the  
779 manuscript and fruitful discussions.

780

781 **Competing Interests**

782 The authors declare no competing interests.  
783

784

785

786 **Funding**

787 This work has been supported by the Swedish Research Council [521-2012-  
788 2037], Swedish Cancer Society [150768], Cancer Research Foundations of  
789 Radiumhemmet [144063] and the Swedish Childhood Cancer Foundation  
790 [PR2015-0009].

792

793

794 **Figure Supplements**

795  
796 Figure 1-Supplement 1: TCAG expression levels and correlation analysis  
797 statistics.

798

799 Figure 1-Supplement 2: Molecular characteristics of miR34a asRNA.

800

801 Figure 2-Supplement 1: A schematic representation of the p1 construct.

802

803 Figure 2-Supplement 2: Evaluating the effects of miR34a asRNA down-  
804 regulation.

805

806 Figure 3-Supplement 1: Physiological relevance of miR34a asRNA  
807 overexpression.

808

809 Figure 3-Supplement 2: Effects of miR34a asRNA overexpression on cyclin  
810 D1.

811

812 Figure 4-Supplement 1: Survival analysis in 17 cancers from TCGA.

813

814 Supplementary Document 1: Evaluating the relationship between miR34a  
815 asRNA and Inc34a.

816

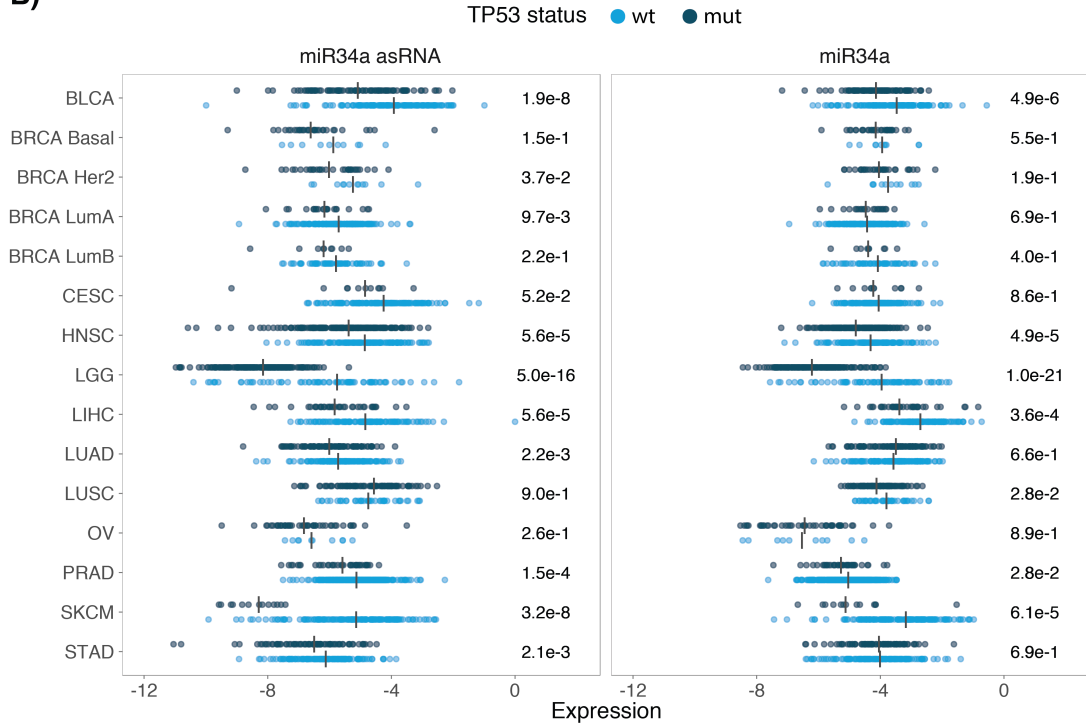
817   Supplementary Document 2: A table of primers used in this study.

818 **Supplementary Figures**

**A)**

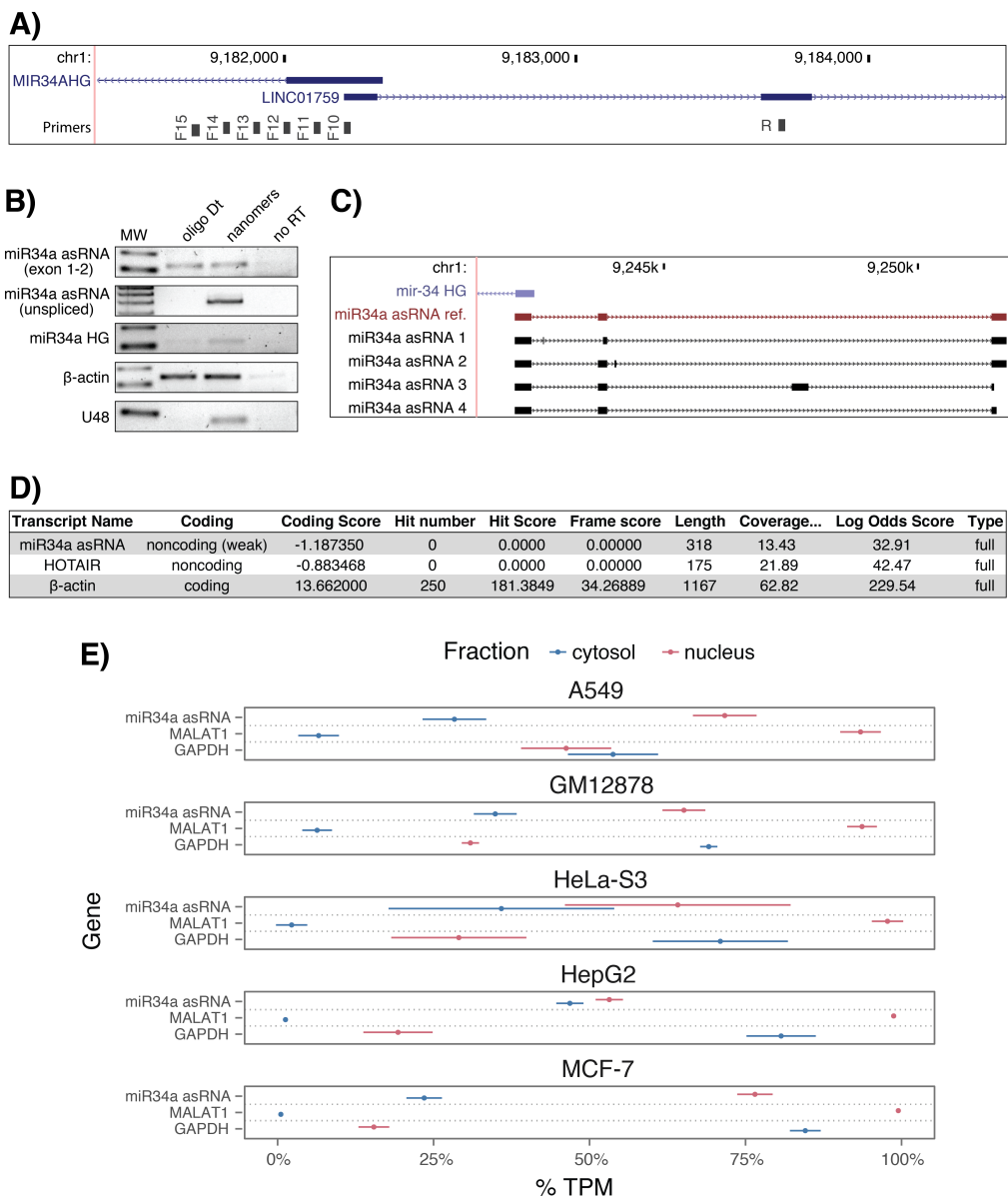
cancer	all n	all rho	all p	TP53wt n	TP53wt rho	TP53wt p	TP53mut n	TP53mut rho	TP53mut p
Adrenocortical carcinoma ( ACC )	10	0.55	1.04e-01	10	0.55	1.04e-01	NA	NA	NA
Bladder Urothelial Carcinoma ( BLCA )	228	0.51	7.89e-17	134	0.45	3.86e-08	94	0.43	1.73e-05
Breast invasive carcinoma ( BRCA ) Basal	42	0.57	9.54e-05	10	0.62	6.02e-02	32	0.57	7.41e-04
Breast invasive carcinoma ( BRCA ) Her2	44	0.15	3.39e-01	12	0.22	4.85e-01	32	0.07	7.10e-01
Breast invasive carcinoma ( BRCA ) LumA	199	0.34	8.22e-07	177	0.34	2.96e-06	22	0.49	2.31e-02
Breast invasive carcinoma ( BRCA ) LumB	70	0.17	1.57e-01	61	0.15	2.53e-01	9	0.17	6.78e-01
Cervical squamous cell carcinoma and endocervical adenocarcinoma ( CESC )	156	0.14	8.37e-02	145	0.16	5.45e-02	11	-0.05	9.03e-01
Head and Neck squamous cell carcinoma ( HNSC )	313	0.54	8.38e-25	123	0.61	0.00e+00	190	0.45	9.68e-11
Kidney Chromophobe ( KICH )	5	0.60	3.50e-01	5	0.60	3.50e-01	NA	NA	NA
Kidney renal clear cell carcinoma ( KIRC )	142	0.35	2.06e-05	141	0.34	4.41e-05	NA	NA	NA
Kidney renal papillary cell carcinoma ( KIRP )	167	0.45	9.16e-10	163	0.45	2.04e-09	4	0.80	3.33e-01
Brain Lower Grade Glioma ( LGG )	271	0.63	9.92e-32	76	0.73	0.00e+00	195	0.39	2.26e-08
Liver hepatocellular carcinoma ( LIHC )	153	0.56	3.64e-14	114	0.52	4.18e-09	39	0.45	3.95e-03
Lung adenocarcinoma ( LUAD )	234	0.28	1.15e-05	128	0.36	2.87e-05	106	0.23	1.91e-02
Lung squamous cell carcinoma ( LUSC )	139	0.23	6.74e-03	42	0.04	7.93e-01	97	0.33	9.91e-04
Ovarian serous cystadenocarcinoma ( OV )	56	0.23	8.37e-02	10	0.84	4.46e-03	46	0.15	3.31e-01
Prostate adenocarcinoma ( PRAD )	413	0.47	1.33e-23	375	0.46	6.13e-21	38	0.45	4.58e-03
Skin Cutaneous Melanoma ( SKCM )	165	0.65	5.43e-21	152	0.61	7.85e-17	13	0.43	1.40e-01
Stomach adenocarcinoma ( STAD )	225	0.37	8.23e-09	145	0.37	5.71e-06	80	0.42	1.03e-04
Thyroid carcinoma ( THCA )	469	0.46	1.07e-25	467	0.46	4.06e-26	NA	NA	NA

**B)**



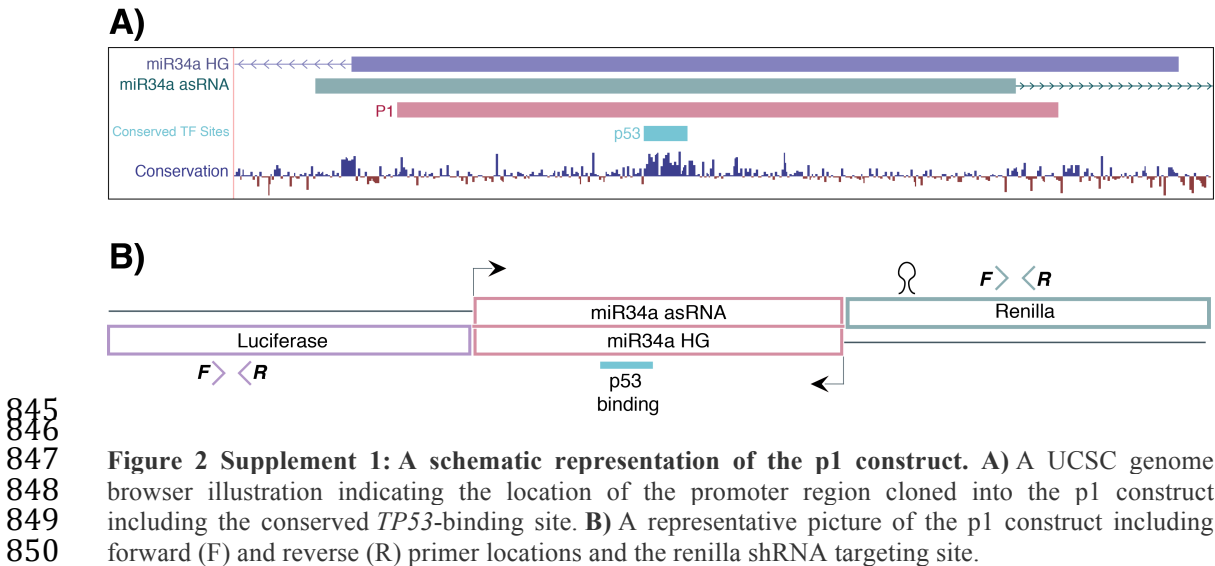
819  
820

**Figure 1 Supplement 1: TCGA normalized expression levels and correlation analysis statistics.**  
**A)** Spearman's rho and p-values (p) from the correlation analysis in Figure 1a between miR34a and miR34a asRNA expression in TP53 wild type (wt) and mutated (mut) samples within TCGA cancer types. NA indicates not applicable, due to a lack of data for the specific group. **B)** Expression levels of *miR34a* and *miR34a* asRNA in *TP53* wt and nonsynonymous mutation samples. Expression was quantified by the log2 ratio of expression of the gene to its maximal expression value. Vertical lines indicate the median. P-values are indicated on the right side of each panel and are derived from comparing the *TP53* wild type samples to the samples with a nonsynonymous mutation using a two-sided Wilcoxon signed rank test. Only samples that had at least 5 samples per comparison were included. In addition, only samples that were diploid at the as miR34a locus and were used for the analysis to avoid copy number bias.

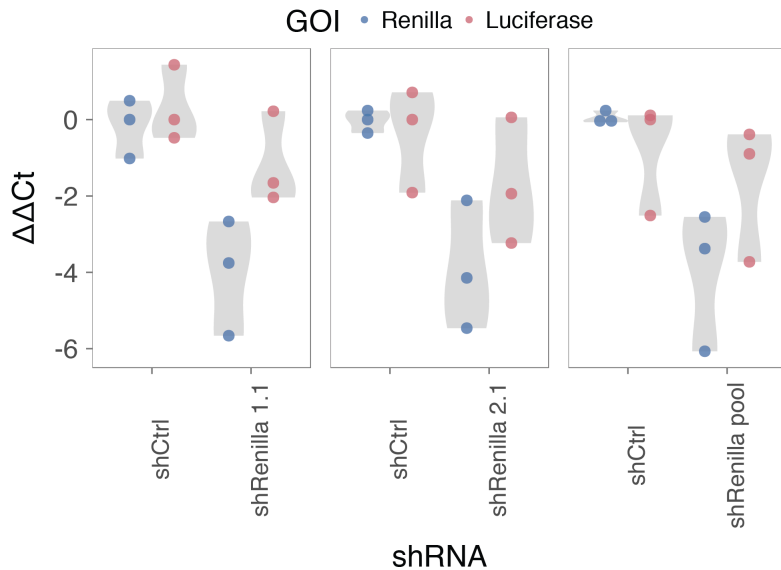


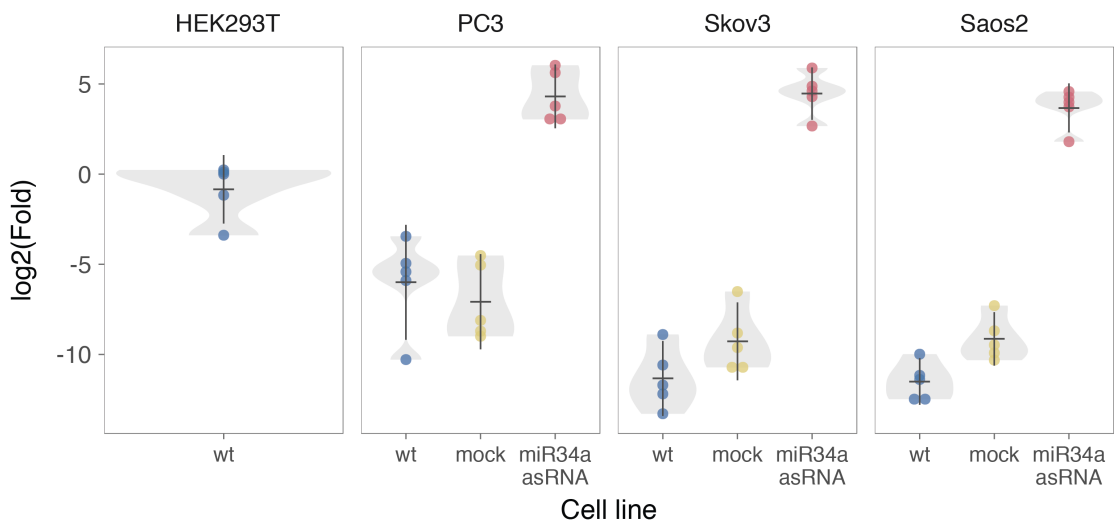
832  
833

834 **Figure 1 Supplement 2: Molecular characteristics of miR34a asRNA.** A) A schematic  
835 representation of the primer placement in the primer walk assay. B) Polyadenylation status of spliced  
836 and unspliced miR34a asRNA in HEK293T cells. C) Sequencing results from the analysis  
837 of miR34a asRNA isoforms in U2OS cells. miR34a AS ref. refers to the full-length transcript as  
838 defined by the 3'-RACE and primer walk assay. D) Analysis of coding potential of the miR34a asRNA  
839 transcript using the Coding-potential Calculator. E) RNAseq data from five fractionated cell lines in  
840 the ENCODE project showing the percentage of transcripts per million (TPM) for miR34a asRNA.  
841 MALAT1 (nuclear localization) and GAPDH (cytoplasmic localization) are included as fractionation  
842 controls. Points represent the mean and horizontal lines represent the standard deviation from two  
843 biological replicates.  
844



853 **Figure 2 Supplement 2: Evaluating the effects of miR34a asRNA down-regulation.** HEK293T  
854 cells were co-transfected with the p1 construct and either shRenilla or shControl. Renilla and  
855 luciferase levels were measured with Q-PCR 48 hours after transfection. Individual points  
856 represent independent experiments with the gray shadow indicating the density of the points.  
857 The experiment was performed in biological triplicate.





858  
859

860 **Figure 3 Supplement 1: Physiological relevance of *miR34a* asRNA overexpression.** Comparison  
861 of *miR34a* asRNA expression in HEK293T cells (high endogenous *miR34a* asRNA), and the wild-type  
862 (wt), mock, and *miR34a* asRNA over-expressing stable cell lines.

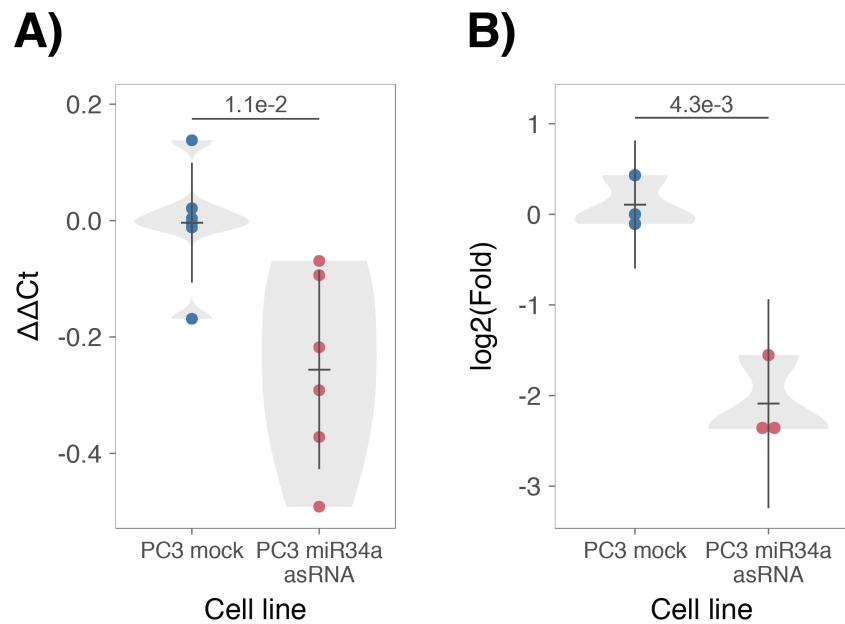
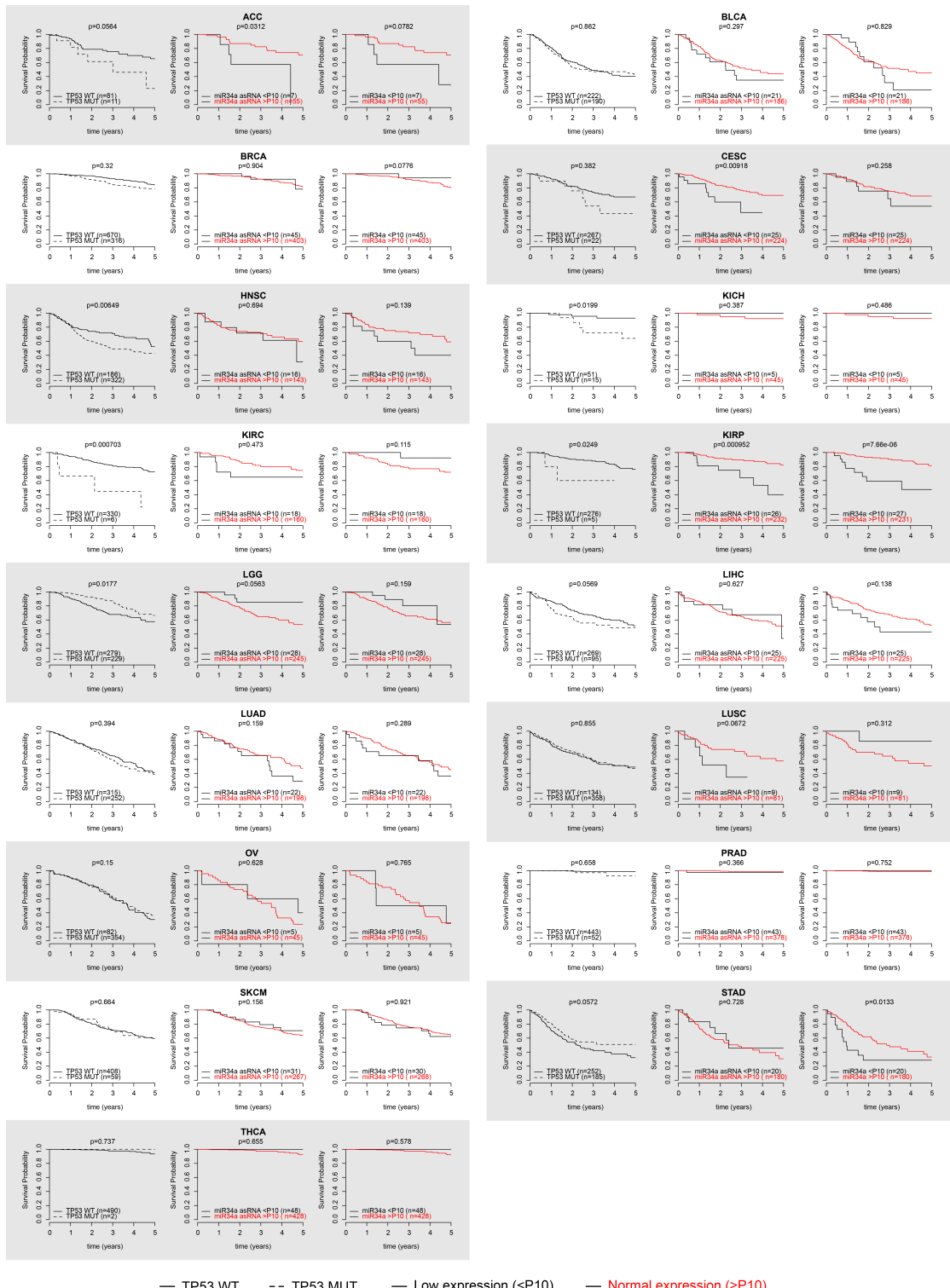


**Figure 3 Supplement 2: Effects of miR34a asRNA overexpression on cyclin D1.** CCND1 expression (A) and western blot quantification of protein levels (B) in *miR34a* asRNA over-expressing PC3 stable cell lines. Experiments were performed in biological sextuplets (A) or triplicates (B).

863  
864  
865  
866  
867



868

869  
870  
871  
872 **Figure 4-Supplement 1: Survival analysis in 17 cancers from TCGA.** Kaplan-Meier survival curves  
comparing the effects of TP53-mutated samples (left), low miR34a asRNA expression (middle) and  
low miR34a expression (right) to control samples in 17 cancer types from TCGA. Low expression was  
defined as TP53 non-mutated samples having expression values in the bottom 10th percentile.

873

874

## 875 References

876

877 Agostini, M., P. Tucci, R. Killick, E. Candi, B. S. Sayan, P. Rivetti di Val Cervo, P.  
878 Nicotera, F. McKeon, R. A. Knight, T. W. Mak and G. Melino (2011). "Neuronal  
879 differentiation by TAp73 is mediated by microRNA-34a regulation of synaptic  
880 protein targets." *Proc Natl Acad Sci U S A* **108**(52): 21093-21098. DOI:  
881 10.1073/pnas.1112061109

882

883 Ahn, Y. H., D. L. Gibbons, D. Chakravarti, C. J. Creighton, Z. H. Rizvi, H. P. Adams, A.  
884 Pertsemlidis, P. A. Gregory, J. A. Wright, G. J. Goodall, E. R. Flores and J. M. Kurie  
885 (2012). "ZEB1 drives prometastatic actin cytoskeletal remodeling by  
886 downregulating miR-34a expression." *J Clin Invest* **122**(9): 3170-3183. DOI:  
887 10.1172/JCI63608

888

889 Allaire, J., Y. Xie, J. McPherson, J. Luraschi, K. Ushey, A. Atkins, H. Wickham, J.  
890 Cheng and W. Chang (2017). rmarkdown: Dynamic Documents for R. R package  
891 version 1.8. <https://CRAN.R-project.org/package=rmarkdown>

892

893 Amarzguioui, M., J. J. Rossi and D. Kim (2005). "Approaches for chemically  
894 synthesized siRNA and vector-mediated RNAi." *FEBS Lett* **579**(26): 5974-5981.  
895 DOI: 10.1016/j.febslet.2005.08.070

896

897 Arnold, J. B. (2017). ggthemes: Extra Themes, Scales and Geoms for 'ggplot2'. R  
898 package version 3.4.0. <https://CRAN.R-project.org/package=ggthemes>

899

900 Ashouri, A., V. I. Sayin, J. Van den Eynden, S. X. Singh, T. Papagiannakopoulos and  
901 E. Larsson (2016). "Pan-cancer transcriptomic analysis associates long non-  
902 coding RNAs with key mutational driver events." *Nature Communications* **7**:  
903 13197. DOI: 10.1038/ncomms13197

904

905 Balbin, O. A., R. Malik, S. M. Dhanasekaran, J. R. Prensner, X. Cao, Y. M. Wu, D.  
906 Robinson, R. Wang, G. Chen, D. G. Beer, A. I. Nesvizhskii and A. M. Chinnaiyan  
907 (2015). "The landscape of antisense gene expression in human cancers." *Genome  
908 Res* **25**(7): 1068-1079. DOI: 10.1101/gr.180596.114

909

910 Boque-Sastre, R., M. Soler, C. Oliveira-Mateos, A. Portela, C. Moutinho, S. Sayols, A.  
911 Villanueva, M. Esteller and S. Guil (2015). "Head-to-head antisense transcription  
912 and R-loop formation promotes transcriptional activation." *Proc Natl Acad Sci U  
913 SA* **112**(18): 5785-5790. DOI: 10.1073/pnas.1421197112

914

915 Chang, T. C., D. Yu, Y. S. Lee, E. A. Wentzel, D. E. Arking, K. M. West, C. V. Dang, A.  
916 Thomas-Tikhonenko and J. T. Mendell (2008). "Widespread microRNA  
917 repression by Myc contributes to tumorigenesis." *Nat Genet* **40**(1): 43-50. DOI:  
918 10.1038/ng.2007.30

919

920 Chang, W. (2014). extrafont: Tools for using fonts. R package version 0.17.  
921 <https://CRAN.R-project.org/package=extrafont>

922

- 923 Chen, J., M. Sun, W. J. Kent, X. Huang, H. Xie, W. Wang, G. Zhou, R. Z. Shi and J. D.  
924 Rowley (2004). "Over 20% of human transcripts might form sense-antisense  
925 pairs." *Nucleic Acids Res* **32**(16): 4812-4820. DOI: 10.1093/nar/gkh818
- 926
- 927 Cheng, J., L. Zhou, Q. F. Xie, H. Y. Xie, X. Y. Wei, F. Gao, C. Y. Xing, X. Xu, L. J. Li and S.  
928 S. Zheng (2010). "The impact of miR-34a on protein output in hepatocellular  
929 carcinoma HepG2 cells." *Proteomics* **10**(8): 1557-1572. DOI:  
930 10.1002/pmic.200900646
- 931
- 932 Chim, C. S., K. Y. Wong, Y. Qi, F. Loong, W. L. Lam, L. G. Wong, D. Y. Jin, J. F. Costello  
933 and R. Liang (2010). "Epigenetic inactivation of the miR-34a in hematological  
934 malignancies." *Carcinogenesis* **31**(4): 745-750. DOI: 10.1093/carcin/bgq033
- 935
- 936 Cole, K. A., E. F. Attiyeh, Y. P. Mosse, M. J. Laquaglia, S. J. Diskin, G. M. Brodeur and  
937 J. M. Maris (2008). "A functional screen identifies miR-34a as a candidate  
938 neuroblastoma tumor suppressor gene." *Mol Cancer Res* **6**(5): 735-742. DOI:  
939 10.1158/1541-7786.MCR-07-2102
- 940
- 941 Conley, A. B. and I. K. Jordan (2012). "Epigenetic regulation of human cis-natural  
942 antisense transcripts." *Nucleic Acids Res* **40**(4): 1438-1445. DOI:  
943 10.1093/nar/gkr1010
- 944
- 945 Consortium, E. P. (2012). "An integrated encyclopedia of DNA elements in the  
946 human genome." *Nature* **489**(7414): 57-74. DOI: 10.1038/nature11247
- 947
- 948 Ding, N., H. Wu, T. Tao and E. Peng (2017). "NEAT1 regulates cell proliferation  
949 and apoptosis of ovarian cancer by miR-34a-5p/BCL2." *Onco Targets Ther* **10**:  
950 4905-4915. DOI: 10.2147/OTT.S142446
- 951
- 952 Djebali, S., C. A. Davis, A. Merkel, A. Dobin, T. Lassmann, A. Mortazavi, A. Tanzer, J.  
953 Lagarde, W. Lin, F. Schlesinger, C. Xue, G. K. Marinov, J. Khatun, B. A. Williams, C.  
954 Zaleski, J. Rozowsky, M. Roder, F. Kokocinski, R. F. Abdelhamid, T. Alioto, I.  
955 Antoshechkin, M. T. Baer, N. S. Bar, P. Batut, K. Bell, I. Bell, S. Chakrabortty, X.  
956 Chen, J. Chrast, J. Curado, T. Derrien, J. Drenkow, E. Dumais, J. Dumais, R.  
957 Duttagupta, E. Falconnet, M. Fastuca, K. Fejes-Toth, P. Ferreira, S. Foissac, M. J.  
958 Fullwood, H. Gao, D. Gonzalez, A. Gordon, H. Gunawardena, C. Howald, S. Jha, R.  
959 Johnson, P. Kapranov, B. King, C. Kingswood, O. J. Luo, E. Park, K. Persaud, J. B.  
960 Preall, P. Ribeca, B. Risk, D. Robyr, M. Sammeth, L. Schaffer, L. H. See, A. Shahab, J.  
961 Skancke, A. M. Suzuki, H. Takahashi, H. Tilgner, D. Trout, N. Walters, H. Wang, J.  
962 Wrobel, Y. Yu, X. Ruan, Y. Hayashizaki, J. Harrow, M. Gerstein, T. Hubbard, A.  
963 Reymond, S. E. Antonarakis, G. Hannon, M. C. Giddings, Y. Ruan, B. Wold, P.  
964 Carninci, R. Guigo and T. R. Gingeras (2012). "Landscape of transcription in  
965 human cells." *Nature* **489**(7414): 101-108. DOI: 10.1038/nature11233
- 966
- 967 Gallardo, E., A. Navarro, N. Vinolas, R. M. Marrades, T. Diaz, B. Gel, A. Quera, E.  
968 Bandres, J. Garcia-Foncillas, J. Ramirez and M. Monzo (2009). "miR-34a as a  
969 prognostic marker of relapse in surgically resected non-small-cell lung cancer."  
970 *Carcinogenesis* **30**(11): 1903-1909. DOI: 10.1093/carcin/bgp219
- 971

- 972 Grossman, R. L., A. P. Heath, V. Ferretti, H. E. Varmus, D. R. Lowy, W. A. Kibbe and  
973 L. M. Staudt (2016). "Toward a Shared Vision for Cancer Genomic Data." N Engl J  
974 Med **375**(12): 1109-1112. DOI: 10.1056/NEJMmp1607591
- 975
- 976 Hunten, S., M. Kaller, F. Drepper, S. Oeljeklaus, T. Bonfert, F. Erhard, A. Dueck, N.  
977 Eichner, C. C. Friedel, G. Meister, R. Zimmer, B. Warscheid and H. Hermeking  
978 (2015). "p53-Regulated Networks of Protein, mRNA, miRNA, and lncRNA  
979 Expression Revealed by Integrated Pulsed Stable Isotope Labeling With Amino  
980 Acids in Cell Culture (pSILAC) and Next Generation Sequencing (NGS) Analyses."  
981 Mol Cell Proteomics **14**(10): 2609-2629. DOI: 10.1074/mcp.M115.050237
- 982
- 983 International Human Genome Sequencing, C. (2004). "Finishing the euchromatic  
984 sequence of the human genome." Nature **431**(7011): 931-945. DOI:  
985 10.1038/nature03001
- 986
- 987 Johnsson, P., A. Ackley, L. Vidarsdottir, W. O. Lui, M. Corcoran, D. Grander and K.  
988 V. Morris (2013). "A pseudogene long-noncoding-RNA network regulates PTEN  
989 transcription and translation in human cells." Nat Struct Mol Biol **20**(4): 440-  
990 446. DOI: 10.1038/nsmb.2516
- 991
- 992 Katayama, S., Y. Tomaru, T. Kasukawa, K. Waki, M. Nakanishi, M. Nakamura, H.  
993 Nishida, C. C. Yap, M. Suzuki, J. Kawai, H. Suzuki, P. Carninci, Y. Hayashizaki, C.  
994 Wells, M. Frith, T. Ravasi, K. C. Pang, J. Hallinan, J. Mattick, D. A. Hume, L. Lipovich,  
995 S. Batalov, P. G. Engstrom, Y. Mizuno, M. A. Faghihi, A. Sandelin, A. M. Chalk, S.  
996 Mottagui-Tabar, Z. Liang, B. Lenhard, C. Wahlestedt, R. G. E. R. Group, G. Genome  
997 Science and F. Consortium (2005). "Antisense transcription in the mammalian  
998 transcriptome." Science **309**(5740): 1564-1566. DOI: 10.1126/science.1112009
- 999
- 1000 Kent, W. J., C. W. Sugnet, T. S. Furey, K. M. Roskin, T. H. Pringle, A. M. Zahler and D.  
1001 Haussler (2002). "The human genome browser at UCSC." Genome Res **12**(6):  
1002 996-1006. DOI: 10.1101/gr.229102. Article published online before print in May  
1003 2002
- 1004
- 1005 Kim, K. H., H. J. Kim and T. R. Lee (2017). "Epidermal long non-coding RNAs are  
1006 regulated by ultraviolet irradiation." Gene **637**: 196-202. DOI:  
1007 10.1016/j.gene.2017.09.043
- 1008
- 1009 Kong, L., Y. Zhang, Z. Q. Ye, X. Q. Liu, S. Q. Zhao, L. Wei and G. Gao (2007). "CPC:  
1010 assess the protein-coding potential of transcripts using sequence features and  
1011 support vector machine." Nucleic Acids Res **35**(Web Server issue): W345-349.  
1012 DOI: 10.1093/nar/gkm391
- 1013
- 1014 Lal, A., M. P. Thomas, G. Altschuler, F. Navarro, E. O'Day, X. L. Li, C. Concepcion, Y.  
1015 C. Han, J. Thiery, D. K. Rajani, A. Deutsch, O. Hofmann, A. Ventura, W. Hide and J.  
1016 Lieberman (2011). "Capture of microRNA-bound mRNAs identifies the tumor  
1017 suppressor miR-34a as a regulator of growth factor signaling." PLoS Genet **7**(11):  
1018 e1002363. DOI: 10.1371/journal.pgen.1002363
- 1019

- 1020 Leveille, N., C. A. Melo, K. Rooijers, A. Diaz-Lagares, S. A. Melo, G. Korkmaz, R.  
1021 Lopes, F. Akbari Moqadam, A. R. Maia, P. J. Wijchers, G. Geeven, M. L. den Boer, R.  
1022 Kalluri, W. de Laat, M. Esteller and R. Agami (2015). "Genome-wide profiling of  
1023 p53-regulated enhancer RNAs uncovers a subset of enhancers controlled by a  
1024 lncRNA." *Nature Communications* **6**: 6520. DOI: 10.1038/ncomms7520
- 1025
- 1026 Liu, C., K. Kelnar, B. Liu, X. Chen, T. Calhoun-Davis, H. Li, L. Patrawala, H. Yan, C.  
1027 Jeter, S. Honorio, J. F. Wiggins, A. G. Bader, R. Fagin, D. Brown and D. G. Tang  
1028 (2011). "The microRNA miR-34a inhibits prostate cancer stem cells and  
1029 metastasis by directly repressing CD44." *Nat Med* **17**(2): 211-215. DOI:  
1030 10.1038/nm.2284
- 1031
- 1032 Memczak, S., M. Jens, A. Elefsinioti, F. Torti, J. Krueger, A. Rybak, L. Maier, S. D.  
1033 Mackowiak, L. H. Gregersen, M. Munschauer, A. Loewer, U. Ziebold, M.  
1034 Landthaler, C. Kocks, F. le Noble and N. Rajewsky (2013). "Circular RNAs are a  
1035 large class of animal RNAs with regulatory potency." *Nature* **495**(7441): 333-  
1036 338. DOI: 10.1038/nature11928
- 1037
- 1038 O'Leary, N. A., M. W. Wright, J. R. Brister, S. Ciufo, D. Haddad, R. McVeigh, B.  
1039 Rajput, B. Robbertse, B. Smith-White, D. Ako-Adjei, A. Astashyn, A. Badretdin, Y.  
1040 Bao, O. Blinkova, V. Brover, V. Chetvernin, J. Choi, E. Cox, O. Ermolaeva, C. M.  
1041 Farrell, T. Goldfarb, T. Gupta, D. Haft, E. Hatcher, W. Hlavina, V. S. Joardar, V. K.  
1042 Kodali, W. Li, D. Maglott, P. Masterson, K. M. McGarvey, M. R. Murphy, K. O'Neill,  
1043 S. Pujar, S. H. Rangwala, D. Rausch, L. D. Riddick, C. Schoch, A. Shkeda, S. S. Storz,  
1044 H. Sun, F. Thibaud-Nissen, I. Tolstoy, R. E. Tully, A. R. Vatsan, C. Wallin, D. Webb,  
1045 W. Wu, M. J. Landrum, A. Kimchi, T. Tatusova, M. DiCuccio, P. Kitts, T. D. Murphy  
1046 and K. D. Pruitt (2016). "Reference sequence (RefSeq) database at NCBI: current  
1047 status, taxonomic expansion, and functional annotation." *Nucleic Acids Res*  
1048 **44**(D1): D733-745. DOI: 10.1093/nar/gkv1189
- 1049
- 1050 Ozsolak, F., P. Kapranov, S. Foissac, S. W. Kim, E. Fishilevich, A. P. Monaghan, B.  
1051 John and P. M. Milos (2010). "Comprehensive polyadenylation site maps in yeast  
1052 and human reveal pervasive alternative polyadenylation." *Cell* **143**(6): 1018-  
1053 1029. DOI: 10.1016/j.cell.2010.11.020
- 1054
- 1055 Polson, A., E. Durrett and D. Reisman (2011). "A bidirectional promoter reporter  
1056 vector for the analysis of the p53/WDR79 dual regulatory element." *Plasmid*  
1057 **66**(3): 169-179. DOI: 10.1016/j.plasmid.2011.08.004
- 1058
- 1059 Rashi-Elkeles, S., H. J. Warnatz, R. Elkon, A. Kupershtain, Y. Chobod, A. Paz, V.  
1060 Amstislavskiy, M. Sultan, H. Safer, W. Nietfeld, H. Lehrach, R. Shamir, M. L. Yaspo  
1061 and Y. Shiloh (2014). "Parallel profiling of the transcriptome, cistrome, and  
1062 epigenome in the cellular response to ionizing radiation." *Sci Signal* **7**(325): rs3.  
1063 DOI: 10.1126/scisignal.2005032
- 1064
- 1065 Raver-Shapira, N., E. Marciano, E. Meiri, Y. Spector, N. Rosenfeld, N. Moskovits, Z.  
1066 Bentwich and M. Oren (2007). "Transcriptional activation of miR-34a  
1067 contributes to p53-mediated apoptosis." *Mol Cell* **26**(5): 731-743. DOI:  
1068 10.1016/j.molcel.2007.05.017

- 1069  
1070 Rinn, J. L., M. Kertesz, J. K. Wang, S. L. Squazzo, X. Xu, S. A. Brugmann, L. H.  
1071 Goodnough, J. A. Helms, P. J. Farnham, E. Segal and H. Y. Chang (2007).  
1072 "Functional demarcation of active and silent chromatin domains in human HOX  
1073 loci by noncoding RNAs." *Cell* **129**(7): 1311-1323. DOI:  
1074 10.1016/j.cell.2007.05.022  
1075  
1076 Rokavec, M., M. G. Oner, H. Li, R. Jackstadt, L. Jiang, D. Lodygin, M. Kaller, D. Horst,  
1077 P. K. Ziegler, S. Schwitalla, J. Slotta-Huspenina, F. G. Bader, F. R. Greten and H.  
1078 Hermeking (2015). "Corrigendum. IL-6R/STAT3/miR-34a feedback loop  
1079 promotes EMT-mediated colorectal cancer invasion and metastasis." *J Clin Invest*  
1080 **125**(3): 1362. DOI: 10.1172/JCI81340  
1081  
1082 Schneider, C. A., W. S. Rasband and K. W. Eliceiri (2012). "NIH Image to ImageJ:  
1083 25 years of image analysis." *Nat Methods* **9**(7): 671-675.  
1084  
1085 Serviss, J. T. (2017). miR34AasRNAproject.  
1086 [https://github.com/GranderLab/miR34a\\_asRNA\\_project](https://github.com/GranderLab/miR34a_asRNA_project)  
1087  
1088 Serviss, J. T., P. Johnsson and D. Grander (2014). "An emerging role for long non-  
1089 coding RNAs in cancer metastasis." *Front Genet* **5**: 234. DOI:  
1090 10.3389/fgene.2014.00234  
1091  
1092 Slabakova, E., Z. Culig, J. Remsik and K. Soucek (2017). "Alternative mechanisms  
1093 of miR-34a regulation in cancer." *Cell Death Dis* **8**(10): e3100. DOI:  
1094 10.1038/cddis.2017.495  
1095  
1096 Stahlhut, C. and F. J. Slack (2015). "Combinatorial Action of MicroRNAs let-7 and  
1097 miR-34 Effectively Synergizes with Erlotinib to Suppress Non-small Cell Lung  
1098 Cancer Cell Proliferation." *Cell Cycle* **14**(13): 2171-2180. DOI:  
1099 10.1080/15384101.2014.1003008  
1100  
1101 Su, X., D. Chakravarti, M. S. Cho, L. Liu, Y. J. Gi, Y. L. Lin, M. L. Leung, A. El-Naggar,  
1102 C. J. Creighton, M. B. Suraokar, I. Wistuba and E. R. Flores (2010). "TAp63  
1103 suppresses metastasis through coordinate regulation of Dicer and miRNAs."  
1104 *Nature* **467**(7318): 986-990. DOI: 10.1038/nature09459  
1105  
1106 Sun, F., H. Fu, Q. Liu, Y. Tie, J. Zhu, R. Xing, Z. Sun and X. Zheng (2008).  
1107 "Downregulation of CCND1 and CDK6 by miR-34a induces cell cycle arrest."  
1108 *FEBS Lett* **582**(10): 1564-1568. DOI: 10.1016/j.febslet.2008.03.057  
1109  
1110 Tarasov, V., P. Jung, B. Verdoodt, D. Lodygin, A. Epanchintsev, A. Menssen, G.  
1111 Meister and H. Hermeking (2007). "Differential regulation of microRNAs by p53  
1112 revealed by massively parallel sequencing: miR-34a is a p53 target that induces  
1113 apoptosis and G1-arrest." *Cell Cycle* **6**(13): 1586-1593. DOI:  
1114 10.4161/cc.6.13.4436  
1115  
1116 Team, R. C. (2017). "R: A Language and Environment for Statistical Computing."  
1117 from <https://www.R-project.org/>.

- 1118  
1119 Therneau, T. M. (2015). A Package for Survival Analysis in S. version 2.38.  
1120 <https://CRAN.R-project.org/package=survival>  
1121  
1122 Turner, A. M., A. M. Ackley, M. A. Matrone and K. V. Morris (2012).  
1123 "Characterization of an HIV-targeted transcriptional gene-silencing RNA in  
1124 primary cells." *Hum Gene Ther* **23**(5): 473-483. DOI: 10.1089/hum.2011.165  
1125  
1126 Vogt, M., J. Munding, M. Gruner, S. T. Liffers, B. Verdoodt, J. Hauk, L.  
1127 Steinstraesser, A. Tannapfel and H. Hermeking (2011). "Frequent concomitant  
1128 inactivation of miR-34a and miR-34b/c by CpG methylation in colorectal,  
1129 pancreatic, mammary, ovarian, urothelial, and renal cell carcinomas and soft  
1130 tissue sarcomas." *Virchows Arch* **458**(3): 313-322. DOI: 10.1007/s00428-010-  
1131 1030-5  
1132  
1133 Wang, L., P. Bu, Y. Ai, T. Srinivasan, H. J. Chen, K. Xiang, S. M. Lipkin and X. Shen  
1134 (2016). "A long non-coding RNA targets microRNA miR-34a to regulate colon  
1135 cancer stem cell asymmetric division." *eLife* **5**. DOI: 10.7554/eLife.14620  
1136  
1137 Wang, L., H. J. Park, S. Dasari, S. Wang, J. P. Kocher and W. Li (2013). "CPAT:  
1138 Coding-Potential Assessment Tool using an alignment-free logistic regression  
1139 model." *Nucleic Acids Res* **41**(6): e74. DOI: 10.1093/nar/gkt006  
1140  
1141 Wang, X., J. Li, K. Dong, F. Lin, M. Long, Y. Ouyang, J. Wei, X. Chen, Y. Weng, T. He  
1142 and H. Zhang (2015). "Tumor suppressor miR-34a targets PD-L1 and functions  
1143 as a potential immunotherapeutic target in acute myeloid leukemia." *Cell Signal*  
1144 **27**(3): 443-452. DOI: 10.1016/j.cellsig.2014.12.003  
1145  
1146 Wickham, H. (2016). gtable: Arrange 'Grobs' in Tables. R package version 0.2.0.  
1147 <https://CRAN.R-project.org/package=gtable>  
1148  
1149 Wickham, H. (2017). scales: Scale Functions for Visualization. R package version  
1150 0.5.0. <https://CRAN.R-project.org/package=scales>  
1151  
1152 Wickham, H. (2017). tidyverse: Easily Install and Load the 'Tidyverse'. R package  
1153 version 1.2.1. <https://CRAN.R-project.org/package=tidyverse>  
1154  
1155 Wickham, L. H. a. H. (2017). rlang: Functions for Base Types and Core R and  
1156 'Tidyverse' Features. R package version 0.1.4. [https://CRAN.R-  
1157 project.org/package=rlang](https://CRAN.R-project.org/package=rlang)  
1158  
1159 Wickham, S. M. B. a. H. (2014). magrittr: A Forward-Pipe Operator for R. R  
1160 package version 1.5. <https://CRAN.R-project.org/package=magrittr>  
1161  
1162 Wilkins, D. gggenes: Draw Gene Arrow Maps in 'ggplot2'. R package version  
1163 0.2.0.9003. <https://github.com/wilkox/gggenes>  
1164  
1165 Xiao, N. (2017). liftr: Containerize R Markdown Documents. R package version  
1166 0.7. <https://CRAN.R-project.org/package=liftr>

- 1167  
1168 Xie, Y. (2017). knitr: A General-Purpose Package for Dynamic Report Generation  
1169 in R. R package version 1.17. <https://yihui.name/knitr/>  
1170  
1171 Yang, P., Q. J. Li, Y. Feng, Y. Zhang, G. J. Markowitz, S. Ning, Y. Deng, J. Zhao, S.  
1172 Jiang, Y. Yuan, H. Y. Wang, S. Q. Cheng, D. Xie and X. F. Wang (2012). "TGF-beta-  
1173 miR-34a-CCL22 signaling-induced Treg cell recruitment promotes venous  
1174 metastases of HBV-positive hepatocellular carcinoma." *Cancer Cell* **22**(3): 291-  
1175 303. DOI: 10.1016/j.ccr.2012.07.023  
1176  
1177 Yap, K. L., S. Li, A. M. Munoz-Cabello, S. Raguz, L. Zeng, S. Mujtaba, J. Gil, M. J.  
1178 Walsh and M. M. Zhou (2010). "Molecular interplay of the noncoding RNA ANRIL  
1179 and methylated histone H3 lysine 27 by polycomb CBX7 in transcriptional  
1180 silencing of INK4a." *Mol Cell* **38**(5): 662-674. DOI: 10.1016/j.molcel.2010.03.021  
1181  
1182 Yu, W., D. Gius, P. Onyango, K. Muldoon-Jacobs, J. Karp, A. P. Feinberg and H. Cui  
1183 (2008). "Epigenetic silencing of tumour suppressor gene p15 by its antisense  
1184 RNA." *Nature* **451**(7175): 202-206. DOI: 10.1038/nature06468  
1185  
1186 Zenz, T., J. Mohr, E. Eldering, A. P. Kater, A. Buhler, D. Kienle, D. Winkler, J. Durig,  
1187 M. H. van Oers, D. Mertens, H. Dohner and S. Stilgenbauer (2009). "miR-34a as  
1188 part of the resistance network in chronic lymphocytic leukemia." *Blood* **113**(16):  
1189 3801-3808. DOI: 10.1182/blood-2008-08-172254  
1190  
1191  
1192  
1193